

# International Journal for Computational Methods in Engineering Science and Mechanics

ISSN: (Print) (Online) Journal homepage: <https://www.tandfonline.com/loi/ucme20>

## Nowcasting prediction of wind speed using computational intelligence and wavelet in Brazil

Pedro Junior Zucatelli, Erick Giovani Sperandio Nascimento, Alex Álisson Bandeira Santos & Davidson Martins Moreira

**To cite this article:** Pedro Junior Zucatelli, Erick Giovani Sperandio Nascimento, Alex Álisson Bandeira Santos & Davidson Martins Moreira (2020) Nowcasting prediction of wind speed using computational intelligence and wavelet in Brazil, International Journal for Computational Methods in Engineering Science and Mechanics, 21:6, 343-369, DOI: [10.1080/15502287.2020.1841335](https://doi.org/10.1080/15502287.2020.1841335)

**To link to this article:** <https://doi.org/10.1080/15502287.2020.1841335>



Published online: 02 Nov 2020.



Submit your article to this journal 



Article views: 206



View related articles 



View Crossmark data 



Citing articles: 8 [View citing articles](#) 



## Nowcasting prediction of wind speed using computational intelligence and wavelet in Brazil

Pedro Junior Zucatelli<sup>a</sup> , Erick Giovani Sperandio Nascimento<sup>b</sup> , Alex Álisson Bandeira Santos<sup>b</sup> , and Davidson Martins Moreira<sup>a,b</sup> 

<sup>a</sup>Technological Center, Federal University of Espírito Santo – UFES, Vitória, Brazil; <sup>b</sup>Manufacturing and Technology Integrated Campus, SENAI CIMATEC, Salvador, Brazil

### ABSTRACT

This work presents a novel investigation on the nowcasting prediction of wind speed for three sites in Bahia, Brazil. For this, it was applied the computational intelligence by supervised machine learning using different artificial neural network technique, which was trained, validated, and tested using time series are derived from measurements that are acquired in towers equipped with anemometers at heights of 100.0, 120.0 and 150.0 m. To define the most efficient ANN, different topologies were tested using MLP and RNN, applying Wavelet packet decomposition (bior, coif, db, dmey, rbior, sym). The best statistical analysis was RNN + discrete Meyer wavelet.

### HIGHLIGHTS

- A new methodology for improving forecast accuracy of wind speed using artificial neural network (ANN) and Wavelet packet decomposition.
- Using machine learning and Wavelet packet decomposition to nowcast wind speed (m/s).
- To predict the wind speed at 100.0 m, 120.0 m and 150.0 m height in tropical region.
- Performance evaluation of Wavelet packet decomposition applying 48 different mother Wavelet functions.
- ANN approach for the estimation of nine types of wind speed time series.
- The proposed hybrid model (ANN + Wavelet packet decomposition) is capable of wind speed forecasting efficiently.

### KEYWORDS

Computational methods; computer science; engineering science and mechanics; machine learning; sustainable energy; wind power

## 1. Introduction

Technological development regarding renewable energy sources with the ultimate goal of reducing environmental pollution is an issue that deserves attention, mainly due to air pollution from high emissions of greenhouse gases into the atmosphere in several nations, which is an issue that has received a global alert. The consequences of global warming are diverse and complex and can cause irreversible damage to humanity. One of the most notable consequences is the melting of the glaciers. The melting of the glaciers generates environmental and social upheavals. This phenomenon alters the temperature of the oceans, causing an environmental imbalance and affecting mainly marine species. Other consequences of global warming are desertification, alteration of the rain regime, intensification of droughts in certain places, water scarcity, an abundance of rain in some

locations, storms, hurricanes, floods, changes in ecosystems, reduction of biodiversity, loss of areas fertile for agriculture.

A renewable energy source means sustainable energy – something that can't run out, or is endless, like the wind [1]. The wind is a plentiful source of energy. Featuring a growing alternative energy source in the global market, wind power has shown rapid development in the past ten years, from 2010 to 2020 [2, 3]. Wind energy shows significant participation in the energy commercialization market and is expected to show exponential growth in the coming years, from 2020 to 2030 [4]. The energy transition can be noticed in the social consciousness globally and in the policies, most countries are adopting, when outlining their energy strategies, e.g. in Brazil and Uruguay. The hybrid models combined with different single models will be an effective way to improve the wind speed

prediction accuracy, agreement of a particular measurement with an accepted standard [5–9].

In meteorology, it is known that the wind results from the movement of the air due to pressure gradients in the atmosphere. The wind flows from the high-pressure regions to the low-pressure regions. The greater the pressure gradient in the atmosphere, the greater the wind speed and, therefore, the greater the wind energy that can be captured by the wind using wind energy conversion machines: wind turbines. Records say that wind speed is the most critical feature of wind power generation. Wind generation and movement are complex due to several physical factors. Among them, the most important factors are the uneven solar heating on the Earth's surface, the Coriolis effect due to the Earth's autorotation, and local geographic conditions. Since wind speed is a random parameter, measured wind speed data is usually treated using statistical methods [10].

A single model is hard to satisfy the accuracy requirement due to the complex characteristics of wind speed. Modern-day grid reliability and security are highly dependent on accurate wind speed and power forecasts. Whereas the nonlinear nature of wind poses challenges in forecasting via traditional methods, supervised machine learning-based hybrid models adequately address this issue. Nowcasting refers to short lead-time weather forecasts. The World Meteorological Organization (WMO) specifies 0 h to 6 h ahead. Nowcasting is usually applied with techniques that differ significantly from normal numerical weather prediction models. In this time range, it is possible to forecast small features such as individual storms with reasonable accuracy [11]. In Brazil, the electric energy trading chamber (CCEE) acts like an operator in the Brazilian electric energy market, aimed at enabling a competitive, sustainable, and safe trading environment. The CCEE promotes discussions and proposes solutions for the development of the national electric sector, making the dialogue between the agents and the instances of formulation of policies and regulation. The institution's focus is on the evolution of the commercialization segment, based on neutrality, liquidity, and symmetry of information. Accounting involves the calculation of the difference between the energy measured and that contracted by an agent, valued at the difference settlement price (PLD) for financial settlement at CCEE. This step is performed based on the marketing rules, taking into account the short-term market exposures, the receipt/payment of system service charges (ESS), the energy reallocation mechanism (MRE) and the consolidation

of results to be settled, including any financial adjustments.

Signal processing techniques have been used in tandem with machine learning methods to improve the forecast accuracy and eliminate the stochastic variations in the time-series. Signal transforms like the Fourier transform, Wavelet transform, and Wavelet packet decomposition are the common algorithms used. A major drawback of using the Fourier transform in wind speed decomposition is the loss of information concerning the time scale, which is overcome by the Wavelet transform. The Wavelet transform captures information of a signal in both time and frequency scales. Since temporal variations hold greater importance in wind speed time-series analysis, the Fourier transform is not preferred [12].

Works such as [13–18] showed results of numerical simulation, and mathematical modeling for short-term wind speed forecasting with artificial intelligence (AI) techniques, especially using multilayer perceptron (MLP) with feedforward and Levenberg-Marquardt backpropagation training algorithm, all with good results achieved, and low associated errors. Wind power prediction is important for the reliability of the electrical system and can help the planning for wind farms. Brazil is ranked 7<sup>th</sup> in the world ranking of wind energy installed capacity, and Bahia is ranked 2<sup>nd</sup> in the Brazilian ranking of wind energy installed capacity (Figure 1). It is worth mentioning that 80% of Brazilian wind farms are in the Northeast, a region that has one of the best winds in the world for producing wind energy. The favorable winds for producing wind energy are more constant, have a stable speed, and do not change direction frequently [19].

The research presented by Zucatelli et al. [16, 17] showed a computation simulation about the short-term wind speed prediction in the tropical region of Mucuri city, Bahia state, Brazil (humid tropical region), using AI by supervised machine learning technique (with neural network architectures) to the hourly time series representative of the site. The authors used MLP, recurrent neural network (RNN) and Wavelets decomposition with Levenberg-Marquardt Backpropagation training algorithm to predict the wind speed for 1 h ahead, and then apply it for 2 h to 12 h ahead.

The study referenced by Zucatelli et al. [14, 18] shows that the short-term wind speed prediction (1 h to 12 h) for Soriano Department (Mercedes is the capital and largest city of the department of Soriano), humid subtropical region in Uruguay, is performed by applying computational intelligence by supervised

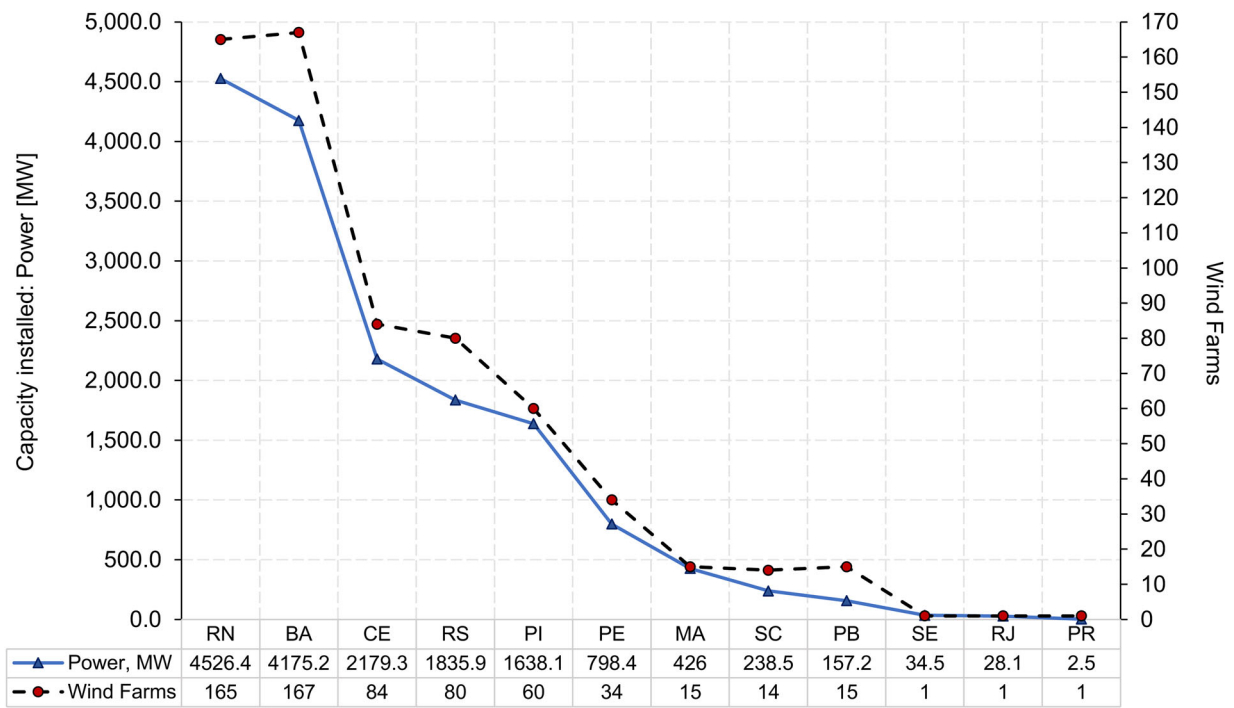


Figure 1. Capacity installed and the number of wind farms in 2020 in Brazilians sites (adapted from [19]).

machine learning by artificial neural network (ANN) technique using anemometer data. The ANN was trained to perform the forecasting of 1 h ahead, and then, using it, the trained network was applied to recursively infer the forecasting for the next hours of the wind speed, the computational complexity is smaller than if it were necessary to train to predict the next 6 h for each input/sample of anemometric data, for example. Different ANN architectures to MLP, RNN, gated recurrent units (GRU), and long short-term memory (LSTM), a deep learning algorithm-based method, are applied for each height (10.0 m, 25.70 m, 81.80 m, and 101.80 m). The statistical results show that the neural networks based on the MLP and LSTM model had the best accuracy when comparing the measured results and the predicted results, in addition to showing more accurate predicted results.

Zucatelli et al. [15] present the nowcasting prediction of wind speed to 6 h ahead, applying AI by supervised machine learning, using MLP and comparing with RNN, and anemometers data collected by an anemometric tower at a height of 100.0 m in Brazil (tropical region) and 101.80 m in Uruguay (subtropical region), both countries located in South America. The proposed method is benchmarked against other computational methods published in the literature and proved to be precise and accurate.

Therefore, this research is a novel investigation that contributes directly to the operation of wind energy

plants for Mucuri, Mucugê, and Esplanada, Bahia, Brazil, with time series of wind derived from measurements that are acquired in three towers equipped with anemometers at heights of 100.0 m, 120.0 m, and 150.0 m. The main contributions of this work can be summarized as follows:

- Nowadays, the application of Wavelet decomposition in weather signals to predict wind speed has been studying in empirical research. Accurate analysis of data is critical to determining the validity of empirical research. The empirical results achieved are promising for the renewable energy market, in this case, wind power, and this is because wind forecasting is important to ensure efficient risk management in wind farms. Nevertheless, there is no scientific methodology for choosing the best Wavelet functions to be applied to temporal wind signals. Therefore, a novel methodology for knowledge discovery is showed using different Wavelet families (48 different mother Wavelet functions), a comparison of Wavelet transform is presented, and different artificial neural network configurations were applied using wind data.
- The proposed model in this paper elucidates the behavior of the wind speed and allows accurate wind speed prediction at three important heights e.g. 100.0 m, 120.0 m, and 150.0 m, and at three important sites i.e. Esplanada, Mucugê, and

- Mucuri (Bahia, Brazil). Short-term wind power prediction can be improved using this computational model to enhance the wind energy quality 6 h ahead (nowcasting). Then a new evaluation of Wavelet families by wind time series decomposition is presented. In this study, the matching relationship between the original wind signal and 48 different mother Wavelet functions was discussed to determine the most suitable mother Wavelet function for the hybrid model.
- c. Research on wind energy forecasting usually focuses on forecast methods, where the design of the input vector is based on anemometer data collected at 10.0 m. The need to use physical equations (i.e. logarithmic profile or power/log law) to calculate the wind at heights greater than 10.0 m adds errors in wind speed and wind direction predictions. Therefore, this study used meteorological measurements measured at 100.0 m, 120.0 m, and 150.0 m to ANN input (training, validation, and test sets). This is important due to the real hub height of the wind turbines in wind farms. The closer the anemometer is placed to the eventual height of the wind turbine hub (e.g. 100.0 m, 120.0 m, and 150.0 m), the more accurately it measures the meteorological variables to which the wind turbine is exposed.
  - d. No previous papers applied artificial intelligence by supervised machine learning and Wavelet decomposition for short-term wind speed prediction for these heights in such a humid tropical climate region (Bahia: 2<sup>nd</sup> in the Brazilian ranking of wind energy installed capacity). It uses an approach to train the model for the next hour forecasting, then recursively inferring the forecasting for the following hours, in addition to applying this AI method targeting short-range wind speed forecasting for these heights in a tropical region. Therefore, the results constitute a significant contribution to the Brazilian electricity market and to neighboring countries, such as Uruguay, which has great wind potential.
  - e. In terms of wind potential, there is a wide variety of wind regimes, i.e. the southern region and the northeast of Brazil. In the southern region, the variability of wind is greater because this region suffers an influence of cold fronts. However, in this region, this difficulty is counterbalanced by greater scientific knowledge and a greater number of measurement systems. In contrast, in the northeast, the climate is tropical, where there are huge gaps in scientific knowledge of wind

behavior in the region and relatively lacking measurement systems. In this sense, the fact that trade winds develop on oceans, impose the need to use wind profiles derived from remote sensing of satellites, in addition to the challenges of complex terrain and coastal regions. These are considered the main scientific frontiers in wind predictability.

The remaining sections of the article are organized as follows: [Section 2](#) describes the methodology, shows the study region, and the data used in this work and provides details of the computational framework used in the computational model, [Section 3](#) presents and discusses obtained results, and [Section 4](#) presents the conclusions of the research, and some suggestions for the future works and studies.

## 2. Methodology

This methodological section presents the anemometers data of the study regions, as well as on the computational model used to wind speed forecasting. The accuracy measures are presented to identify the quality of the adjustments produced by the models. To reach the objective of the present work was adopted the computational intelligence model by supervised machine learning and Wavelet packet decomposition. This computational method is called supervised machine learning ([Figure 2](#)) because the process of an algorithm learning from the training dataset can be thought of as an expert supervising the learning process. It knows the correct answers, the algorithm iteratively makes forecasts on the training data and is corrected by the expert. When the computational algorithm achieves an acceptable level of performance, the machine learning stops.

At this point, it is important to mention that the Bahia state is consolidating the position of the largest Brazilian pole of investments in wind energy, as well as becoming an international reference in this area. Numerous investments have been made by new companies, generating job opportunities and income for the population, including a positive impact in needy regions. A new production chain, focused on wind energy, was successfully implemented in the state and continues to expand, boosting the economy as a whole. Wind energy has become a good alternative to diversification and expansion of the Brazilian electric matrix [[20](#)]. It should be noted that the advancement of technology in wind energy has allowed the installation of turbines at high levels, requiring knowledge of

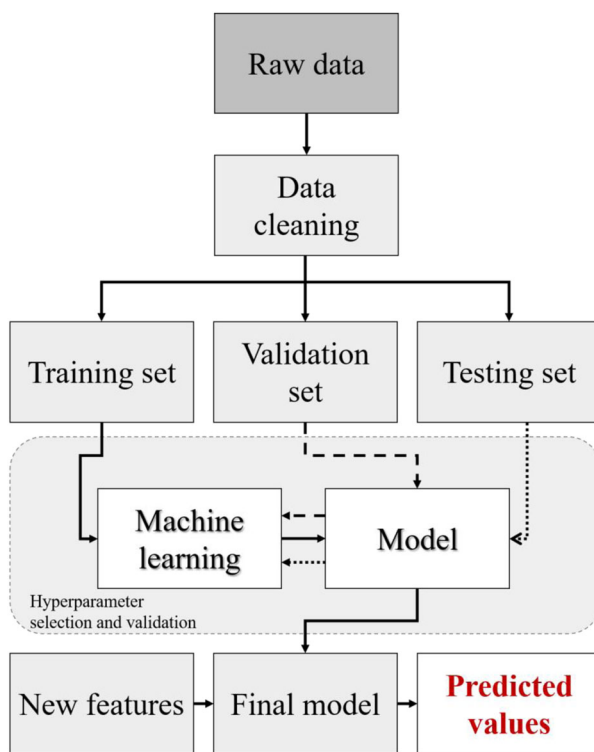


**Figure 2.** Schematic diagram of the supervised learning.

the wind potential at ever greater heights. To validate the estimates and disseminate the installation of wind farms in the state of Bahia, four anemometric towers of 150.0 m height were installed in locations with promising winds, in the cities of Esplanada, Mucugê, Mucuri, and Casa Nova. The anemometric towers installed in Esplanada, Mucugê, and Mucuri are the most important, their anemometric data recorded well represent the climatic diversity of the state of Bahia, and, therefore, contemplate this case study.

The Esplanada city is located in the microregion of the north coast of Bahia with an altitude of 140.0 m concerning the sea level and it has a territorial area of 1,299.35 km<sup>2</sup>, approximately. Its characteristic biome is the Atlantic Forest. The Esplanada's anemometric tower is 40.0 km from the sea, with latitude 11°47'45" S, and longitude 37°56'42" W. The Mucugê city is at an altitude of 984.0 m concerning the sea level and is one of the municipalities belonging to *Chapada Diamantina*, the central region of the state of Bahia, characterized by being a mountainous region and it has a territorial area of 2,462.15 km<sup>2</sup>, approximately. Its characteristic biome is the caatinga. The anemometric tower of Mucugê has located approximately 280.0 km from the Bahia coast, with a latitude of 13°00'18" S, and longitude of 41°22'15" W. The Mucuri city is located at an altitude of 7.0 m concerning the sea level and it has a territorial area of 1,787.62 km<sup>2</sup>, approximately. Its characteristic biome

is the Atlantic Forest. The Mucuri's anemometer tower is located in a coastal plain, at a distance of 340.0 m from the sea, with latitude 18°05'09" S, and longitude 39°33'03" W (see Figure 3), south region of Bahia. The data observed at intervals of 20 in 20 seconds were converted to hourly values, being realized the means of the original measures measured in 1 hour (60 min).

The time series used in the models consists of 744 records in total (100%), corresponding to hourly mean data for each of the period between April 28, 2016, until May 29, 2016 (site: Esplanada), September 07, 2016, until October 07, 2016 (site: Mucugê), and November 30, 2015, until December 31, 2015 (site: Mucuri), see Figures 4–6. The wind database that will be used in this study is characterized by data on speed, direction, temperature, relative humidity, and barometric pressure.

The frequencies distributions of wind speed data are shown in Figures 7–9, and a descriptive statistic regarding wind speed at different sites is shown in Table 1.

The Weibull distribution is important, especially for reliability and maintainability analysis. The probability density function  $f(v)$  is given by the following Equation (1):

$$f(v) = \frac{k}{c} \left(\frac{v}{c}\right)^{k-1} \cdot e^{-\left(\frac{v}{c}\right)^k} \quad (1)$$

where  $v$  = is the wind speed [m/s];  $k$  = is the Weibull shape factor [unitless];  $c$  = is the Weibull scale parameter [m/s]. In this work, to determine the shape ( $k$ ) and scale ( $c$ ) parameters of the Weibull probability density function did apply Justus Empirical Method following Lysen equations, i.e.  $k = (\sigma/\bar{v})^{-1.086}$  and  $c = [\bar{v}(0.568 + 0.433/k) - 1/k]$  where  $\sigma$  is the standard deviation [m/s] and  $\bar{v}$  is the mean wind speed [m/s].

The training set with 550 recorded hours (average hourly values of the wind speed [m/s], wind direction [°], air temperature [°C], air humidity [%], and air pressure [Bar]) was used for the models' training (44.35%), and validation (29.57%). The prediction set

- Esplanada: 05/21/2016 at 7:00 a.m. until 05/29/2016 at 8:00 a.m.,
- Mucugê: 09/29/2016 at 10:00 p.m. until 10/07/2016 at 11:00 p.m., and
- Mucuri: 12/23/2015 at 12:00 p.m. until 12/31/2015 at 1:00 p.m.

consisting of 194 data (26.08%) was used to verify their accuracy during the prediction stage. The software used to program and perform this computational

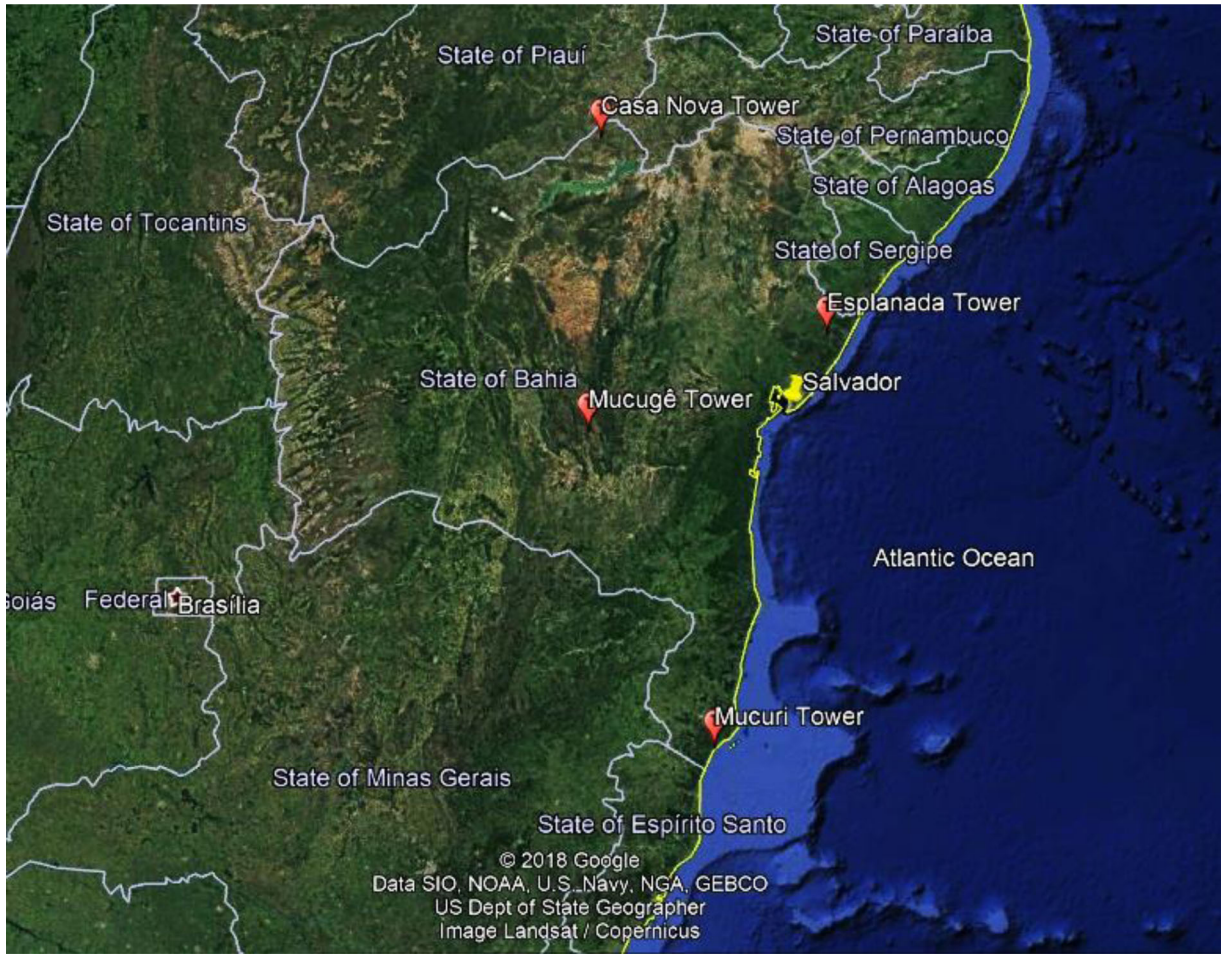


**Figure 3.** Location of Esplanada, Mucugê and Mucuri Towers in Bahia, Brazil.

procedure was Matlab, the core configuration of the personal computer includes Intel Core i7-7500U processors running at 2.90 GHz, and a 64-bit system with 8 GB of RAM, and the proposed ANN architectures to be analyzed are the following ones (see Table 2).

The ANN architecture depends on the number of input features being analyzed. In architecture 1, the input features are day, month, year, hour, and important meteorological parameters: wind speed [m/s], wind direction [ $^{\circ}$ ], air temperature [ $^{\circ}\text{C}$ ], air humidity [%], and air pressure [Bar]; in architecture 2, the value depends on the Wavelet level applied to wind speed decomposition.

Haykin [21] explain that a neuron is an information-processing unit that is fundamental to the operation of a neural network. In mathematical terms, in this paper we may describe a neuron  $k$  by writing the following pair of equations:

$$u_k = \sum_{j=1}^m w_{kj}x_j \quad (2)$$

and

$$y_k = \varphi(u_k + b_k) \quad (3)$$

where  $x_1, x_2, \dots, x_m$  are the input signals;  $w_{k1}, w_{k2}, \dots, w_{kn}$  are the synaptic weights of neuron  $k$ ;  $u_k$  is the linear combiner output due to the input signals;  $b_k$  is the bias;  $\varphi(\bullet)$  is the activation function, and  $y_k$  is the output signal of neuron.

A MLP (Figure 10) is an ANN composed of more than one perceptron. They are composed of an input layer to receive the signal, an output layer that makes a decision or prediction about the input, and between these two, an arbitrary number of hidden layers that are the true computational mechanism of MLP. Multilayer perceptron with a hidden layer can approximate any continuous function. Recurrent networks (Figure 11), on the other hand, take as input not only the example of the current entry it sees but also what it perceived earlier in time. The decision of a recurring network reached in time step  $t-1$  affects the decision that will reach a moment later in time step  $t$ . Thus, RNN has two sources of input, the present, and the recent past, which combine to

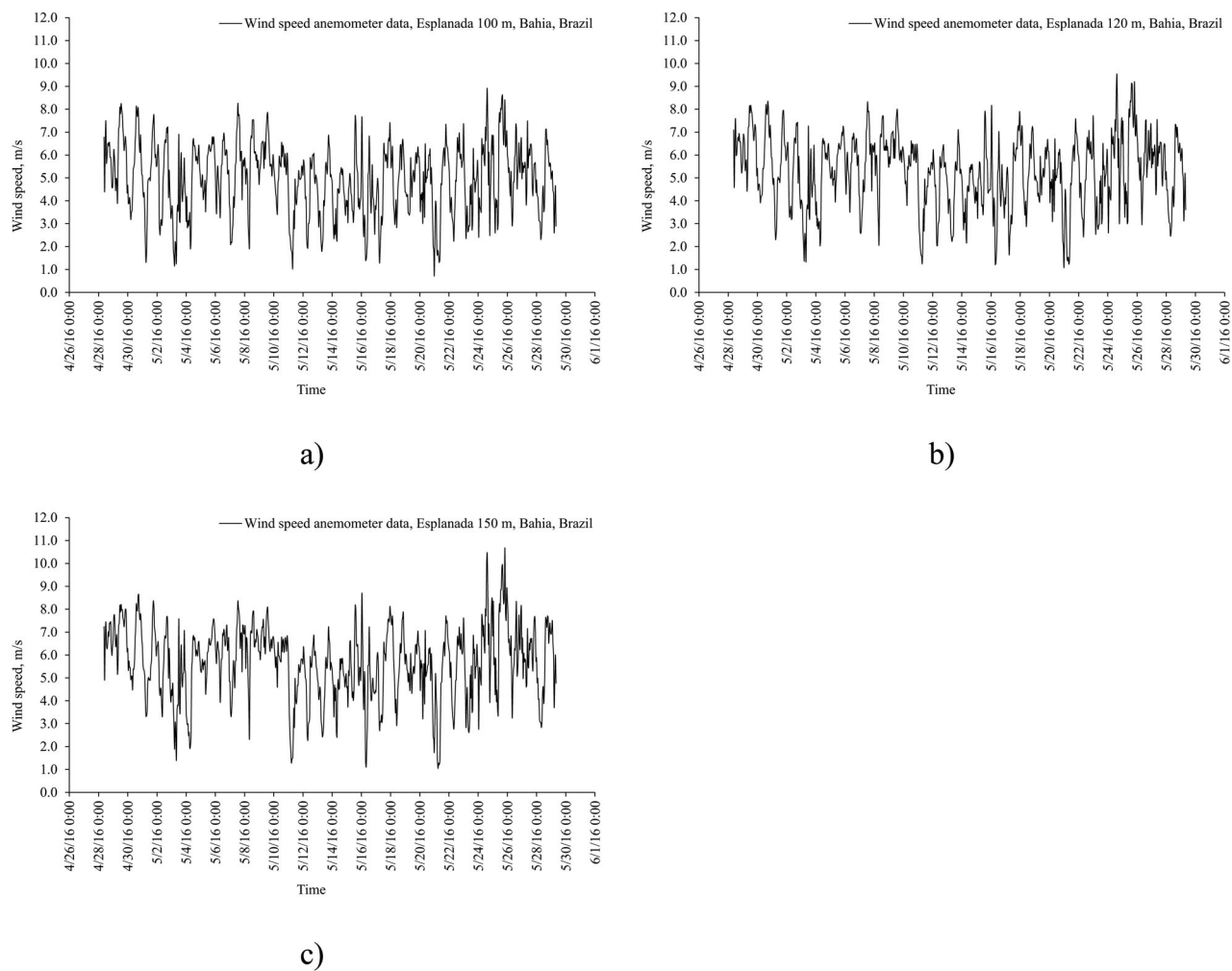


**Figure 4.** Wind speed anemometer data, site: Esplanada 100.0 m (a), 120.0 m (b), and 150.0 m (c).

determine how they respond to new data, according to Haykin [21].

After collecting the anemometric data at each site, the data is preprocessed to ascertain, for example, the presence of *not a number* (or *nan*) and to transform the records into hourly averages. The discrete Wavelet transform using different families is then applied to the selected data set. The high-pass filter results in the detailed coefficients and the low-pass filter results in the approximate coefficients. For these anemometers' signals, the low-frequency content is the most important part, because it is what gives the signal its identity. Thus, the objective is to compare the performance of the approximate coefficients with the original signal to ascertain the maintenance of the energy of the decomposed signal. With the results of this comparison, the most efficient family of Wavelets in this process is evaluated and chosen. After this step, the technology for predicting the approximate and detailed coefficients is applied using supervised machine learning using artificial neural networks. After predicting these

coefficients, the wind speed signal needs to be reconstructed, so that it can be compared with the original signal. The aim is to evaluate the Wavelet before applying computational intelligence. Since the published works perform empirical tests without a scientific methodology for assessing discrete Wavelet families before applying the forecast method. Figure 12 shows a flowchart of the Wavelet decomposition strategy and computational intelligence.

The Wavelet decomposition strategy was applied using mothers' functions Biorthogonal (bior), Reverse biorthogonal (rbio), Coiflet (coif), Daubechies (db), discrete Meyer (dmey), and Symlet (sym). Hybrid models arising from the filtering of anemometric signals through Wavelet decompositions and computational intelligence have been developed with efficiency in the forecast results.

Daubechies [22] teach that a Wavelet transform is a tool that cuts up data or functions or operators into different frequency components, and then studies each component with a resolution matched to its scale. The

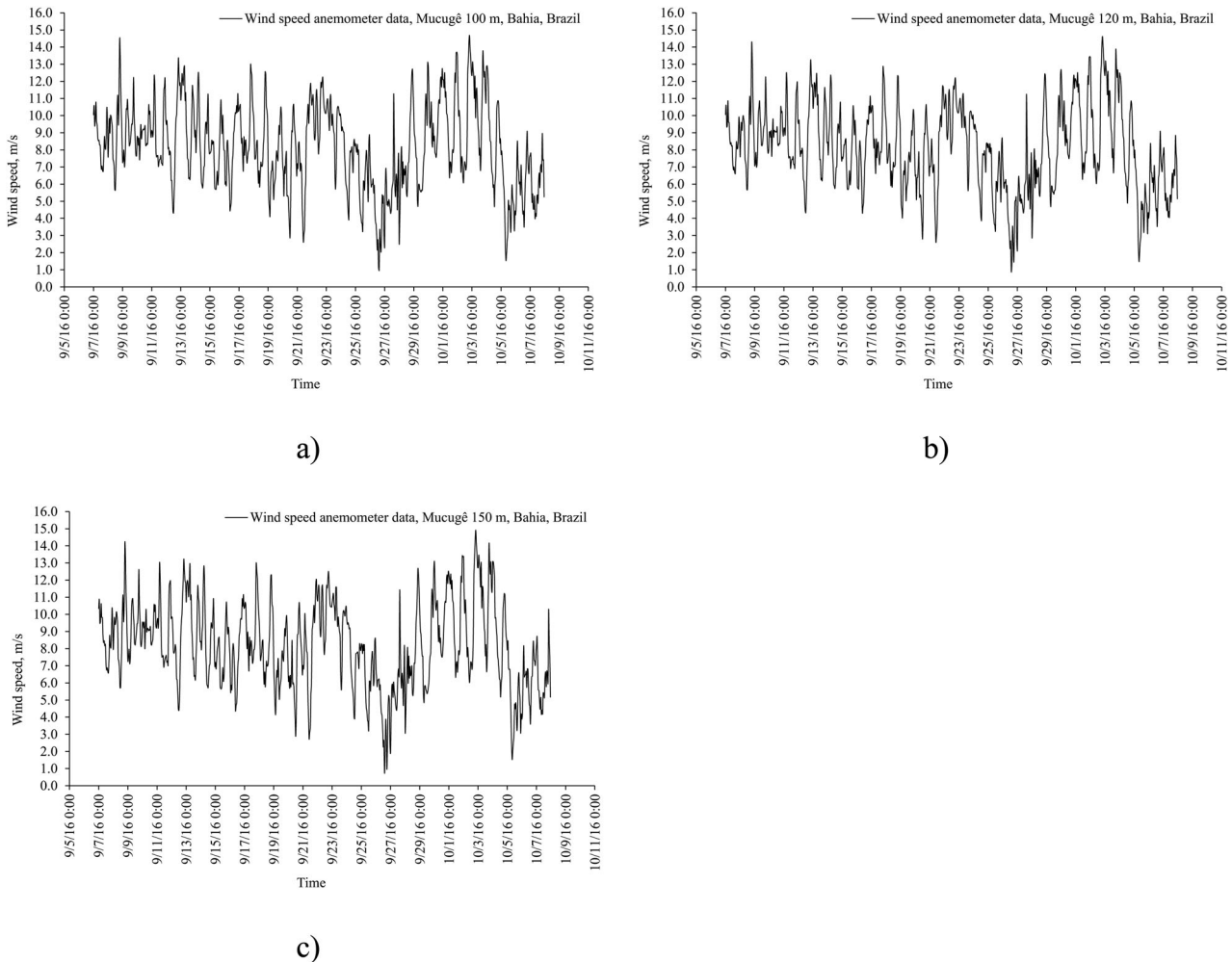


**Figure 5.** Wind speed anemometer data, site: Mucugê 100.0 m (a), 120.0 m (b), and 150.0 m (c).

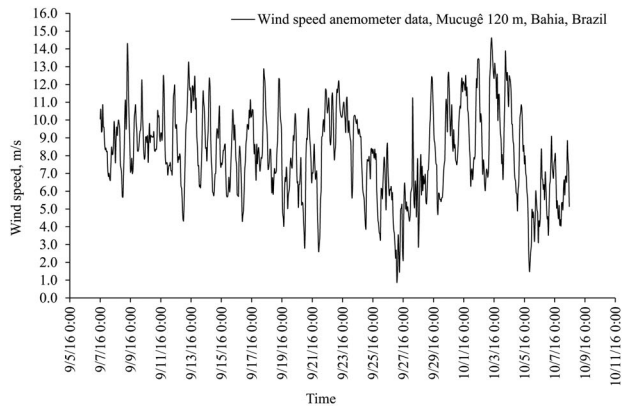
Wavelet transform of a signal evolving in time depends on two variables: frequency (or scale) and time. Wavelets provide a tool for time-frequency localization. In many applications, given a signal  $f(t)$  (for the moment, we assume that  $t$  is a continuous variable), one is interested in its frequency content locally in time. The standard Fourier transform is given by the following Equation (4):

$$(\mathcal{F}f)(\omega) = \frac{1}{\sqrt{2\pi}} \int dt e^{-i\omega t} f(t) \quad (4)$$

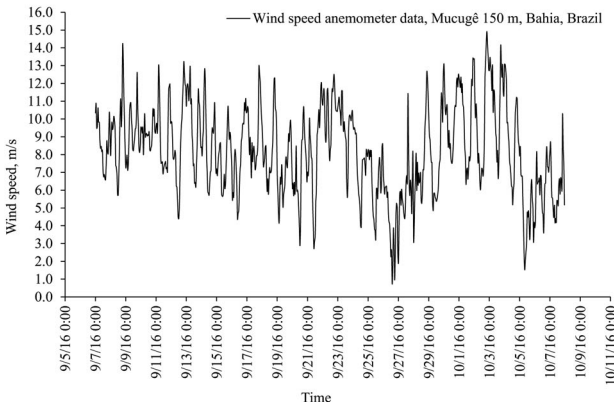
also gives a representation of the frequency content of  $f$ , but information concerning time-localization of, e.g., high-frequency bursts cannot be read off easily from  $\mathcal{F}f$ . Time-localization can be achieved by first windowing the signal  $f$ , so as to cut off only a well-localized slice of  $f$ , and then taking its Fourier transform:

$$(T^{win}f)(\omega, t) = \int ds f(s) g(s - t) e^{-i\omega s} \quad (5)$$

where  $f = \text{function}$ ;  $t = \text{time}$ ;  $\omega = \text{frequency}$ ;  $g = \text{window function}$ .



b)



c)

This is the windowed Fourier transform, which is a standard technique for time-frequency localization. It is even more familiar to signal analysts in its discrete version, where  $t$  and  $\omega$  are assigned regularly spaced values:  $t = nt_0$ ,  $\omega = m\omega_0$ , where  $m, n$  range over  $\mathbb{Z}$ , and  $\omega_0, t_0 > 0$  are fixed. Then Equation (5) becomes

$$T_{m,n}^{win}(f) = \int ds f(s) g(s - nt_0) e^{-im\omega_0 s} \quad (6)$$

for fixed  $n$ , the  $T_{m,n}^{win}(f)$  correspond to the Fourier coefficients of  $f(\bullet)g(\bullet - nt_0)$ . If, for instance,  $g$  is compactly supported, then it is clear that with appropriately chosen  $\omega_0$ , the Fourier coefficients  $T_{m,n}^{win}(f)$  are sufficient to characterize and, if need be, to reconstruct  $f(\bullet)g(\bullet - nt_0)$ . Changing  $n$  amounts to shifting the "slices" by steps of  $t_0$  and its multiples, allowing the recovery of all of  $f$  from the  $T_{m,n}^{win}(f)$ . The windowed Fourier transform provides thus a description of  $f$  in the time-frequency plane.

The idea of the Wavelet transform, first put forward by a geophysicist Jean Moret in 1982 for seismic wave

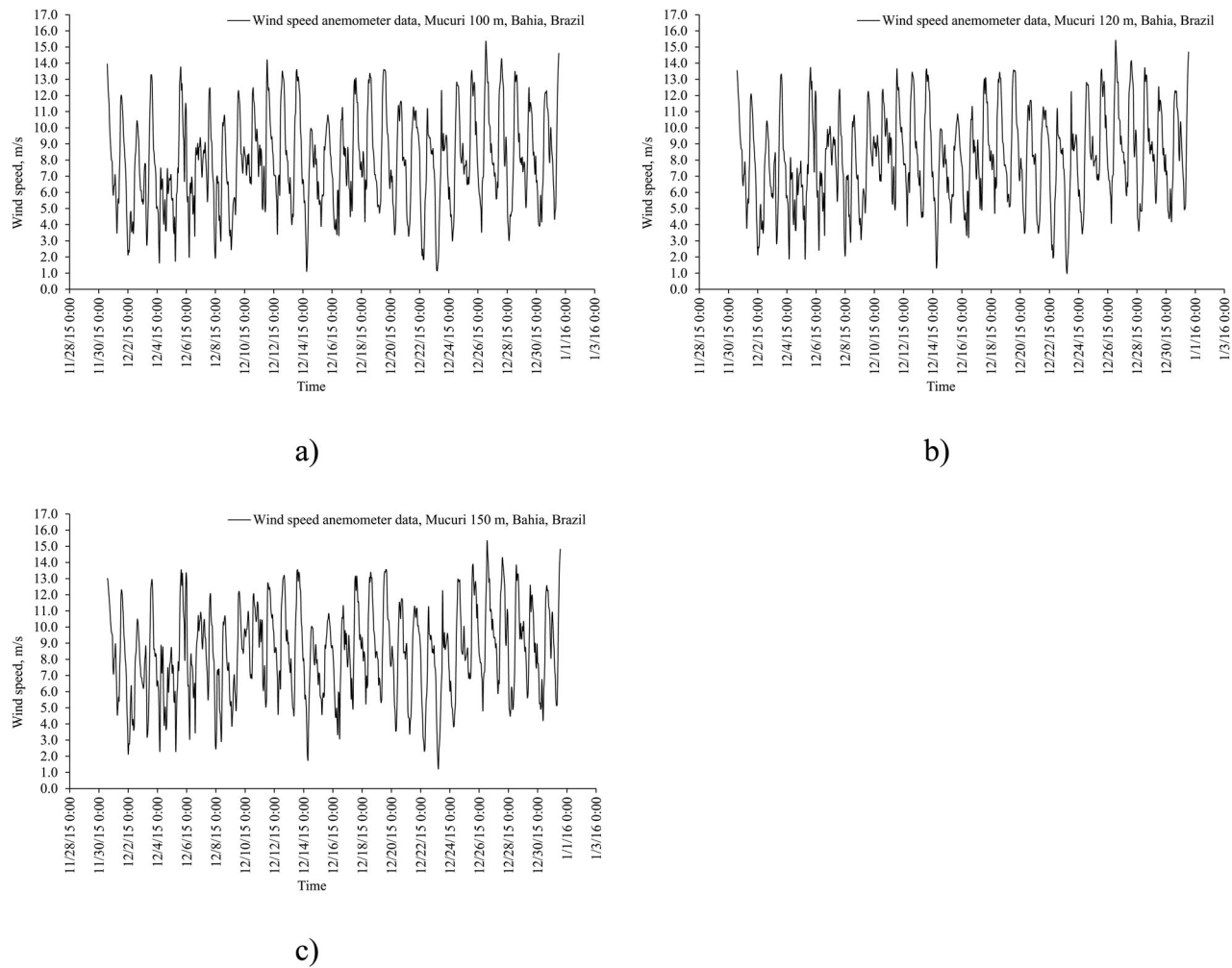


**Figure 6.** Wind speed anemometer data, site: Mucuri 100.0 m (a), 120.0 m (b), and 150.0 m (c).

analysis [22], can be categorized as the continuous wavelet transform (CWT) and discrete wavelet transform (DWT). The continuous Wavelet involves the continuous scaling and time-shifting of the mother Wavelet. The high scaling (low-pass filter) gives approximate information about the signal ( $A_1, A_2, \dots, A_n$ ), whereas low scaling (high-pass filter) gives a detailed information of the signal ( $d_1, d_2, \dots, d_n$ ). The Wavelet transform provides a similar time-frequency description, with a few important differences. The Wavelet transform formulas analogous to (5) and (6) are,

$$(T^{wav}f)(a, b) = |a|^{-1/2} \int dt f(t) \psi\left(\frac{t-b}{a}\right) \quad (7)$$

and

$$T_{m,n}^{wav}(f) = a_0^{-m/2} \int dt f(t) \psi(a_0^{-m}t - nb_0) \quad (8)$$

in both cases, we assume that  $\psi$  satisfies,  $\int dt \psi(t) = 0$ . Equation (8) is again obtained from (7) by restricting  $a, b$  to only discrete values:  $a = a_0^m$ ,  $b = nb_0a_0^m$  in this case,

with  $m, n$  ranging over  $\mathbb{Z}$ , and  $a_0 > 1$ ,  $b_0 > 0$  fixed. One similarity between the Wavelet and windowed Fourier transforms is clear: both (5) and (7) take the inner products of  $f$  with a family of functions indexed by two labels,  $g^{w,t}(s) = e^{iws}g(s-t)$  in (5), and  $\psi^{a,b}(s) = |a|^{-1/2} \psi\left(\frac{s-b}{a}\right)$  in (7). The functions  $\psi^{a,b}$  are called *Wavelets*; the function  $\psi$  is sometimes called *mother Wavelet*. Daubechies [22] notes that  $\psi$  and  $g$  are implicitly assumed to be real, even though this is by no means essential; if they are not, then complex conjugates have to be introduced in (5), (7). There exist many different types of the Wavelet transform, all starting from the basic formulas (7), (8). In these notes we will distinguish between: i) The continuous Wavelet transform (7); and ii) The discrete Wavelet transform (8).

The Meyer Wavelet ( $\hat{\psi}$ ) and scaling function ( $\hat{\phi}$ ) are defined in the frequency domain. Daubechies [22] explain that both  $\hat{\psi}$  and  $\hat{\phi}$  are defined in the frequency domain, starting with an auxiliary function ( $\nu$ ). Then,

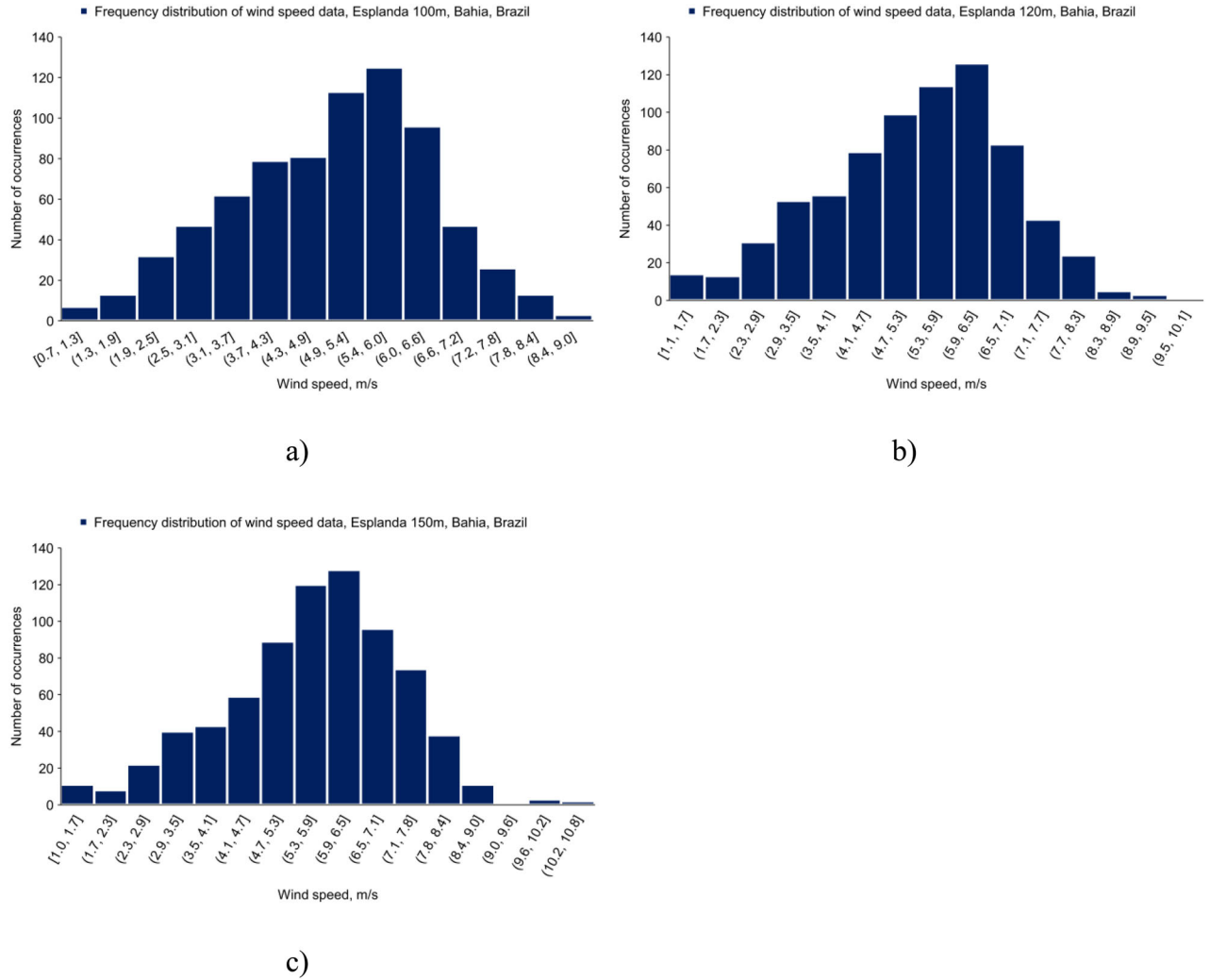


**Figure 7.** Frequency distribution of wind speed data, Esplanada 100.0 m (a), 120.0 m (b), and 150.0 m (c).

the Meyer Wavelet function is represented by Equations (9)–(11), i.e.

$$\hat{\psi}(\omega) = (2\pi)^{-1/2} e^{i\omega/2} \sin \left[ \frac{\pi}{2} \nu \left( \frac{3}{2\pi} |\omega| - 1 \right) \right] \text{ if } \frac{2\pi}{3} \leq |\omega| \leq \frac{4\pi}{3} \quad (9)$$

$$\hat{\psi}(\omega) = (2\pi)^{-1/2} e^{i\omega/2} \cos \left[ \frac{\pi}{2} \nu \left( \frac{3}{4\pi} |\omega| - 1 \right) \right] \text{ if } \frac{4\pi}{3} \leq |\omega| \leq \frac{8\pi}{3} \quad (10)$$

$$\hat{\psi}(\omega) = 0 \text{ if } |\omega| \notin \left[ \frac{2\pi}{3}, \frac{8\pi}{3} \right] \quad (11)$$

and scaling function by Equations (12)–(14),

$$\hat{\phi}(\omega) = (2\pi)^{-1/2} \text{ if } |\omega| \leq \frac{2\pi}{3} \quad (12)$$

$$\hat{\phi}(\omega) = (2\pi)^{-1/2} \cos \left[ \frac{\pi}{2} \nu \left( \frac{3}{2\pi} |\omega| - 1 \right) \right] \text{ if } \frac{2\pi}{3} \leq |\omega| \leq \frac{4\pi}{3} \quad (13)$$

$$\hat{\phi}(\omega) = 0 \text{ if } |\omega| > \frac{4\pi}{3} \quad (14)$$

All ANN (MLP or RNN) were trained with Levenberg-Marquardt backpropagation training algorithm, to predict the wind speed for 1 h ahead, and then apply it for 2 h to 6 h ahead. The Levenberg–Marquardt optimization algorithm exhibits fast convergence speed and applies the Hesse and Jacobian matrices to solve multidimensional optimization problems. The approach to training and validating the model for the next hour wind speed prediction, then recursively inferring the wind speed forecasting for the following hours is showed in Figures 13 and 14.

Therefore, the ANN was trained to perform the wind speed forecasting 1 h ahead, using it, the trained ANN was applied to recursively infer the forecasting

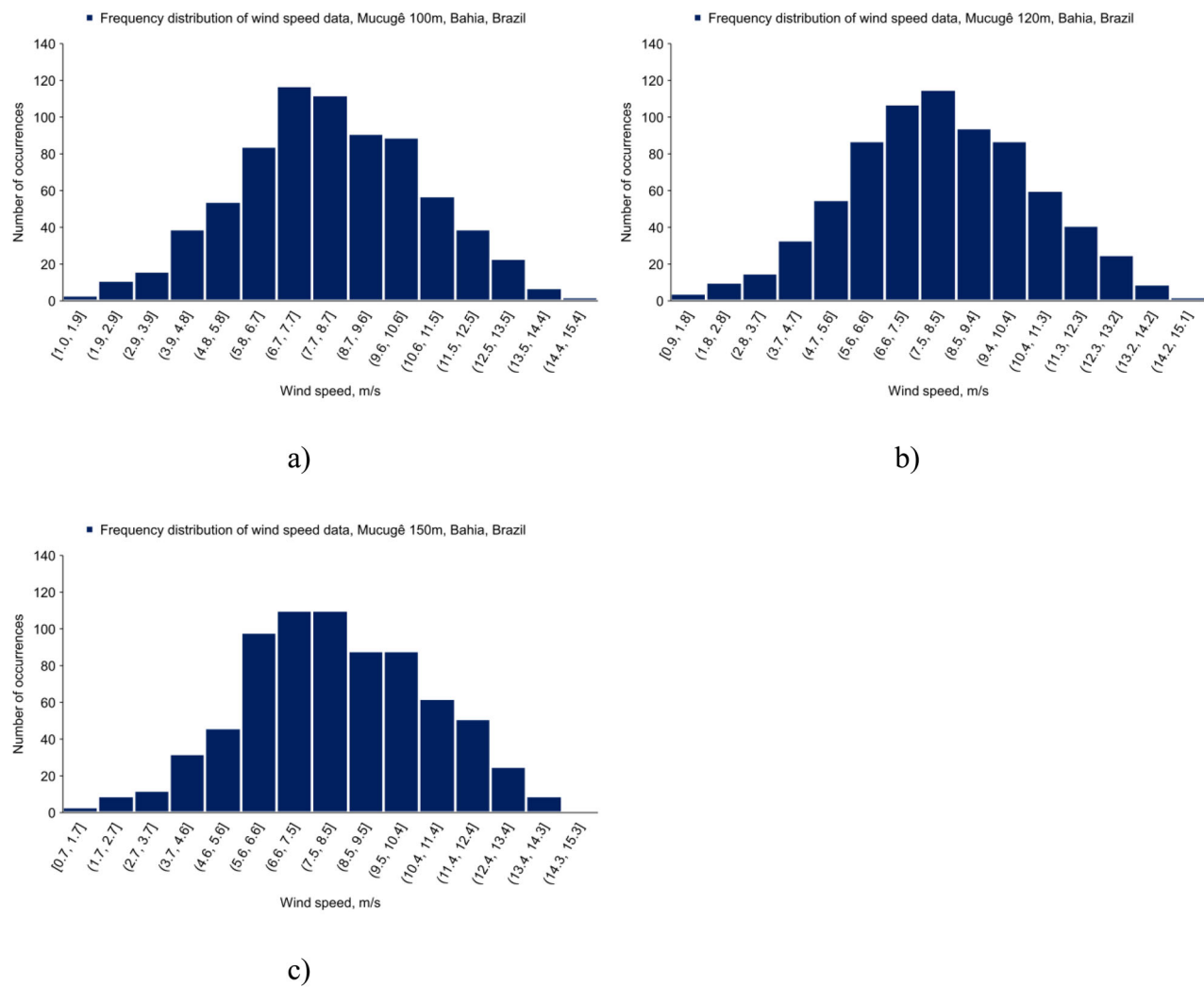


Figure 8. Frequency distribution of wind speed data, Mucugê 100.0 m (a), 120.0 m (b), and 150.0 m (c).

for the next hours of the wind speed. The computational cost of this methodology, as applied in [14–18], is smaller than if it were necessary to train to predict the next  $n$ th hour for each input or sample of anemometric data. Then, to perform the prediction, the first phase is to identify what ANN topology can better perform the wind speed forecasting 1 h ahead for each height and each site. Afterward, this predicted wind speed value is assigned as input for the *second-hour* forecasting. So, it is calculated the forecast of the wind speed for the *second hour*. This computational procedure is repeated until the  $n$ th hour of the forecasting is reached. In this hybrid model (ANN + Wavelet decomposition), the result of the wind speed forecasting is the sum of the predicted detail and approximation components. In this study, the activation functions were hyperbolic tangent function (sigmoidal function: this function accepts both real and

complex inputs) for all hidden layers, and the linear function to the output layer. Results and discussions are presented in the next section.

### 3. Results and discussions

For being able to measure the accuracy of the forecasted values provided by the tool, the error ( $e_t$ ) calculated through Equation (15) was used in this work. This is the method that is commonly used to analyze the efficiency of an ANN. The statistical treatment employed in the results is mean squared error (MSE), root mean squared error (RMSE), Pearson's correlation coefficient (Equations 16–18), and percentage of data of factor of two (Fac2). For these statistical indicators, values close to 0.0 (zero) are adequate for the MSE, RMSE, and values close to 1.0 (one) are adequate for the Pearson. Values close to 100% are adequate for the Fac2. In other words, is a fraction of

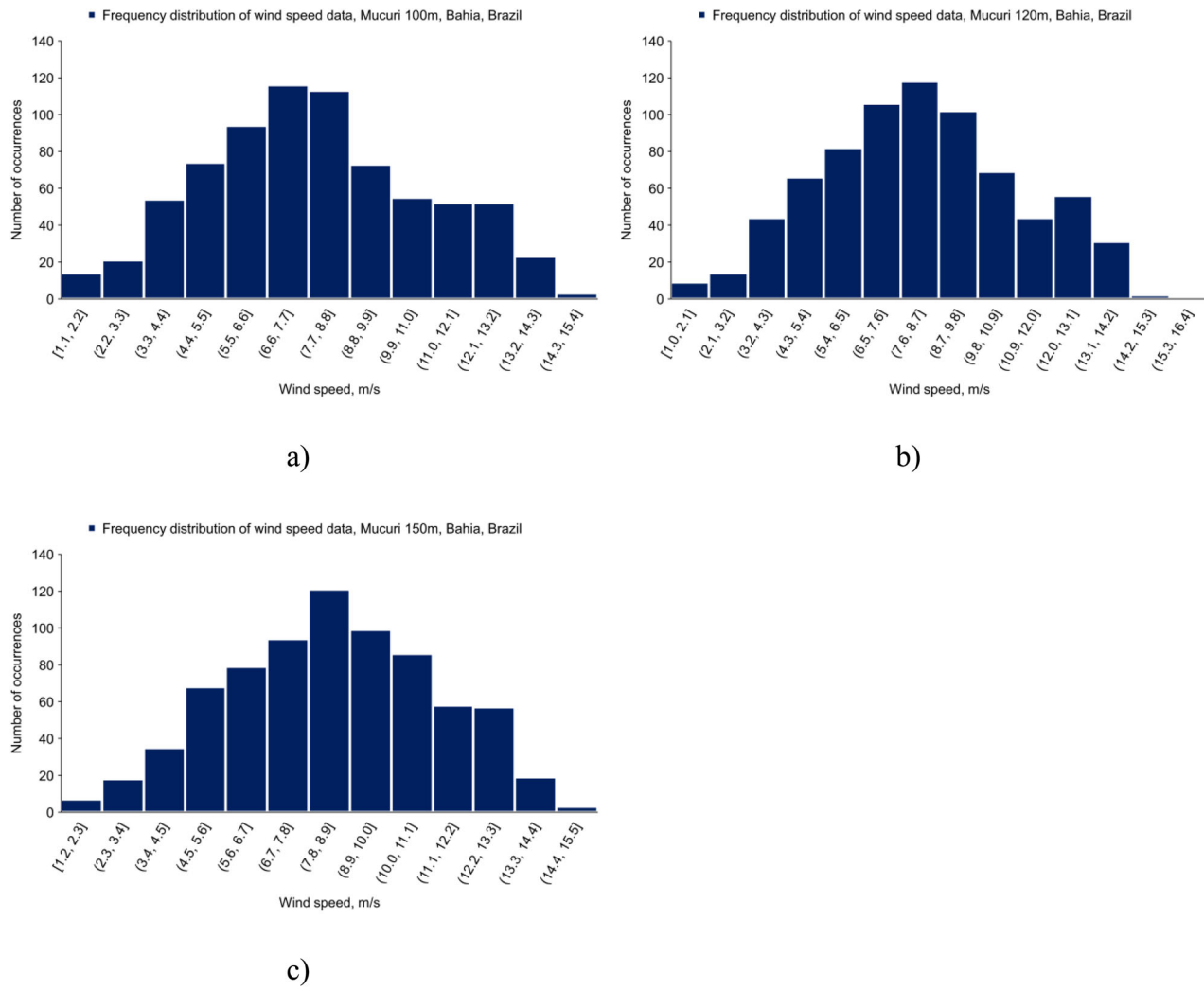


**Figure 9.** Frequency distribution of wind speed data, Mucuri 100.0 m (a), 120.0 m (b), and 150.0 m (c).

**Table 1.** Descriptive statistics regarding wind speed.

| Sites     | Anemometer height [m] | Arithmetic mean of wind speed [m/s] | Variance [ $m^2/s^2$ ] | Standard deviation [m/s] |
|-----------|-----------------------|-------------------------------------|------------------------|--------------------------|
| Esplanada | 100.0                 | 4.956                               | 2.333                  | 1.527                    |
|           | 120.0                 | 5.285                               | 2.382                  | 1.543                    |
|           | 150.0                 | 5.673                               | 2.518                  | 1.587                    |
| Mucugê    | 100.0                 | 8.159                               | 6.158                  | 2.481                    |
|           | 120.0                 | 8.090                               | 6.021                  | 2.453                    |
|           | 150.0                 | 8.192                               | 6.254                  | 2.500                    |
| Mucuri    | 100.0                 | 7.905                               | 8.534                  | 2.921                    |
|           | 120.0                 | 8.127                               | 8.066                  | 2.840                    |
|           | 150.0                 | 8.440                               | 7.586                  | 2.754                    |

**Table 2.** MLP and RNN architectures.

| MLP and RNN configuration (config.) and layer | Architecture 1<br>MLP:<br>input layer | Architecture 2<br>RNN + Wavelets:<br>input layer | 1 <sup>st</sup> hidden layer | 2 <sup>nd</sup> hidden layer | Output layer |
|---|---------------------------------------|--|------------------------------|------------------------------|--------------|
| Config. 1                                     | 9 neurons                             | 8 neurons  | 9 neurons                    | –                            | 1 neuron     |
| Config. 2                                     | 9 neurons                             | 8 neurons  | 6 neurons                    | –                            | 1 neuron     |
| Config. 3                                     | 9 neurons                             | 8 neurons  | 3 neurons                    | –                            | 1 neuron     |
| Config. 4                                     | 9 neurons                             | 8 neurons  | 1 neuron                     | –                            | 1 neuron     |
| Config. 5                                     | 9 neurons                             | 8 neurons  | 9 neurons                    | 6 neurons                    | 1 neuron     |
| Config. 6                                     | 9 neurons                             | 8 neurons  | 6 neurons                    | 3 neurons                    | 1 neuron     |
| Config. 7                                     | 9 neurons                             | 8 neurons  | 1 neuron                     | 1 neuron                     | 1 neuron     |

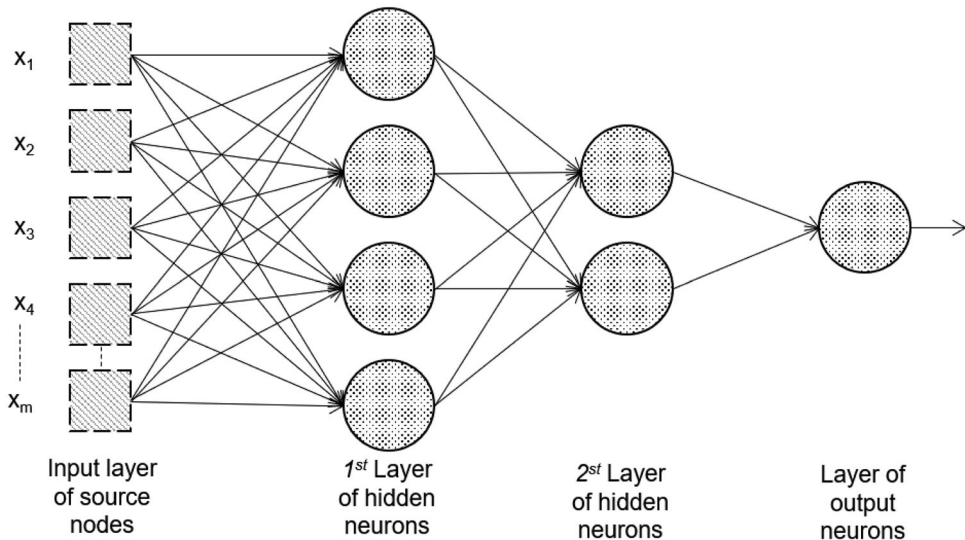


**Figure 10.** Fully connected feedforward or acyclic network with two hidden layers and one output layer.

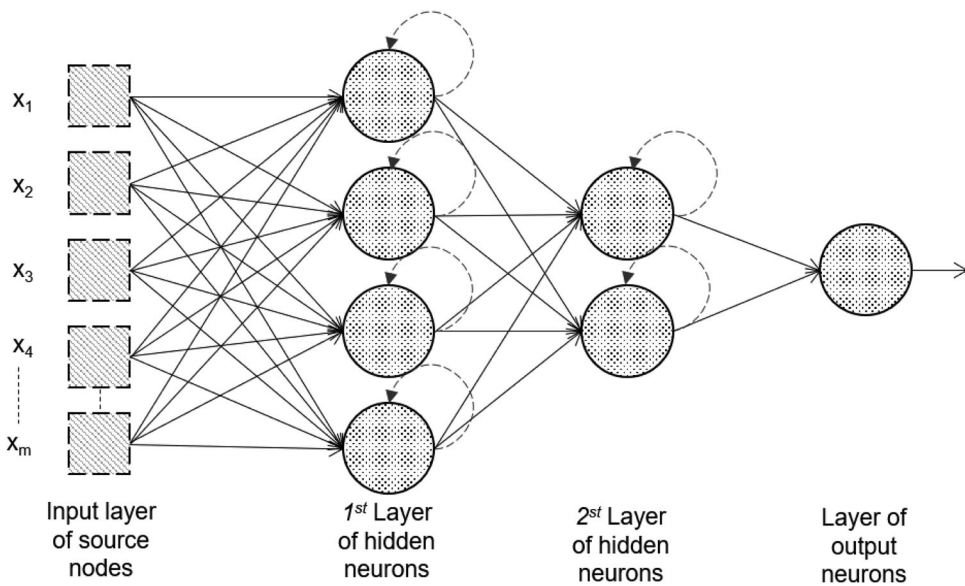


**Figure 11.** Recurrent network with hidden neurons.

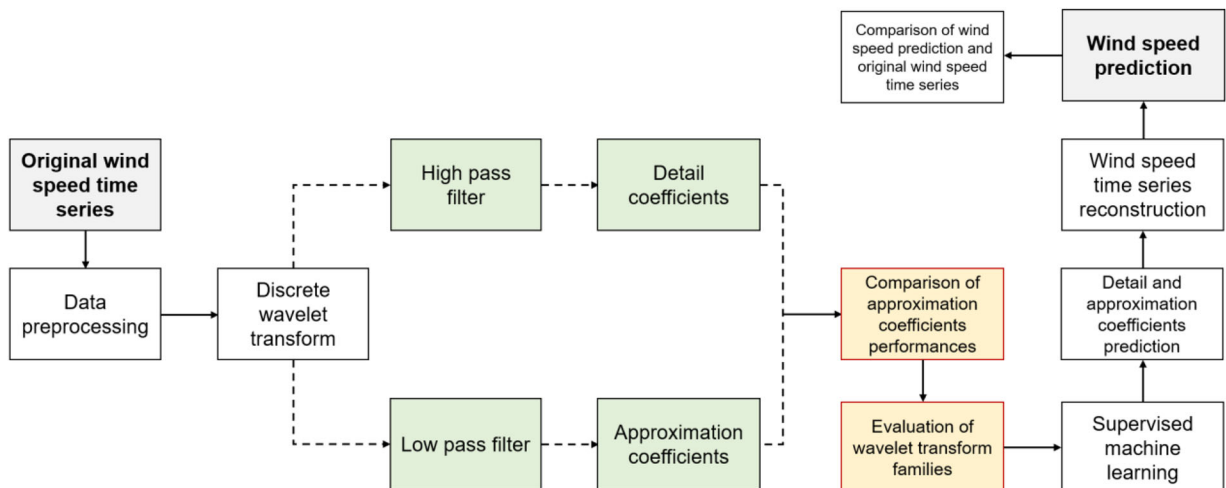


**Figure 12.** Flowchart of the wavelet decomposition strategy.

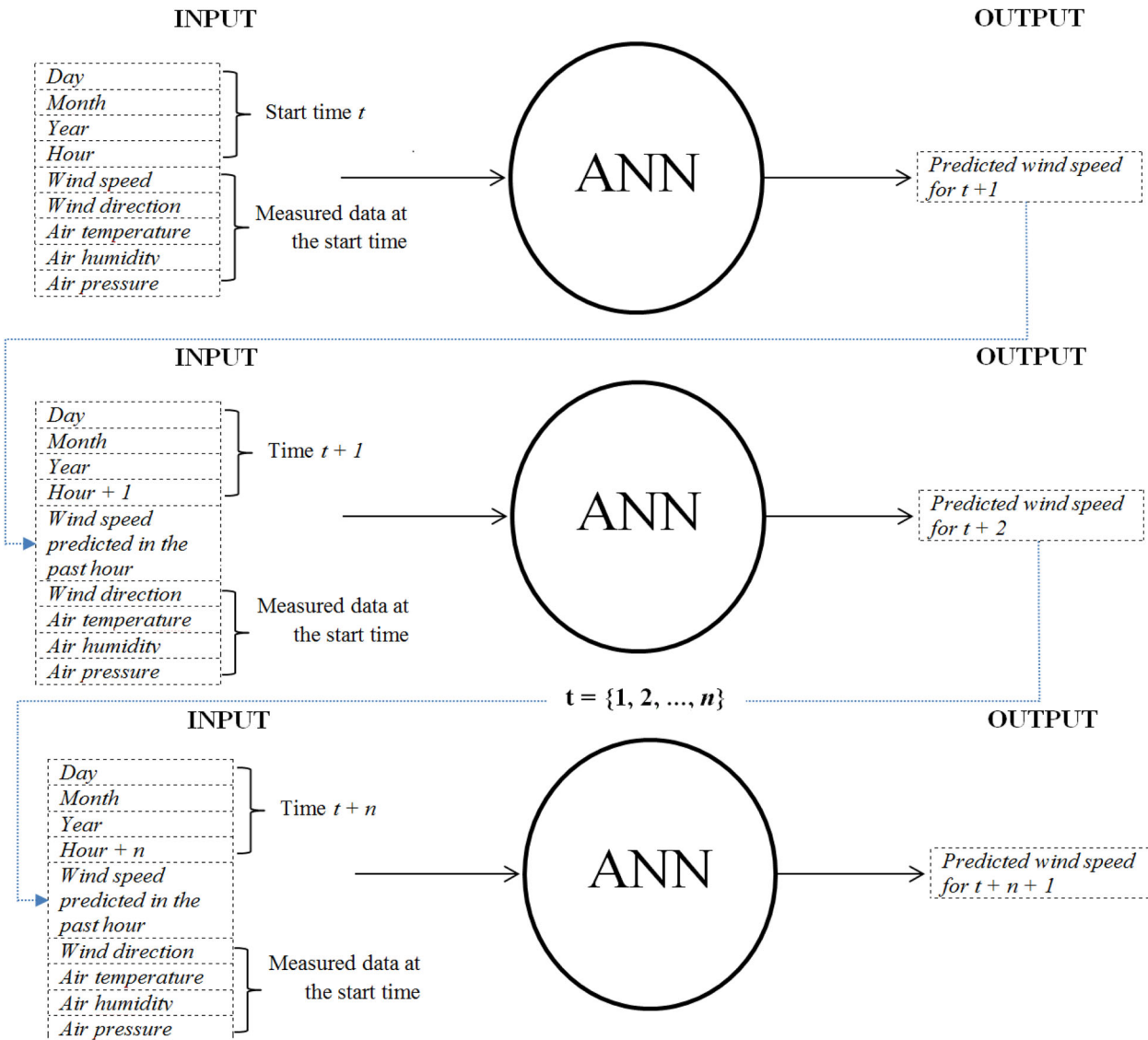


**Figure 13.** Flowchart of the procedure using MLP.

data [%] for  $0.50 \leq (\text{simulated wind speed}/\text{observed wind speed}) \leq 2.0$ .

$$e_t = o_t - f_t \quad (15)$$

$$MSE = \frac{1}{n} \sum_{t=1}^n e_t^2 \quad (16)$$

$$RMSE = \sqrt{\frac{1}{n} \sum_{t=1}^n e_t^2} \quad (17)$$

$$Pearson = \frac{\sum_{t=1}^n (o_t - \bar{o})(f_t - \bar{f})}{\sqrt{\sum_{t=1}^n (o_t - \bar{o})^2 \sum_{t=1}^n (f_t - \bar{f})^2}} \quad (18)$$

where:  $t$  = time;  $n$  = number of samples;  $e_t$  = error;  $o_t$  = observed value;  $f_t$  = forecasted value;  $\bar{o}$  = is the mean of all observed values;  $\bar{f}$  = is the mean of all forecasted values.

**Table 3** presents the Weibull shape factor and the Weibull scale parameter. **Figures 15–17** show Weibull distribution density versus wind speed to all sites and all anemometer height. Sites characterized by very steady winds (like tropical trade wind environments) may have a Weibull shape factor value as high as 3.0 or 4.0.

To find out which family of Wavelets (Daubechies, Biorthogonal, Reverse biorthogonal, Coiflets, Symlets, or discrete Meyer) would present more precision in the decomposition of anemometric signals, in this study, a comparison and a statistical evaluation were analyzed between the approximate level 1 decomposed signal (or A1 signal by Wavelet decomposition) and the original wind speed time series. **Figures 18–24** show the results achieved from this comparison. The Wavelet discrete Meyer family (dmey) demonstrates greater precision in the decomposition of the signals collected in Esplanada, Mucugê, and Mucuri.

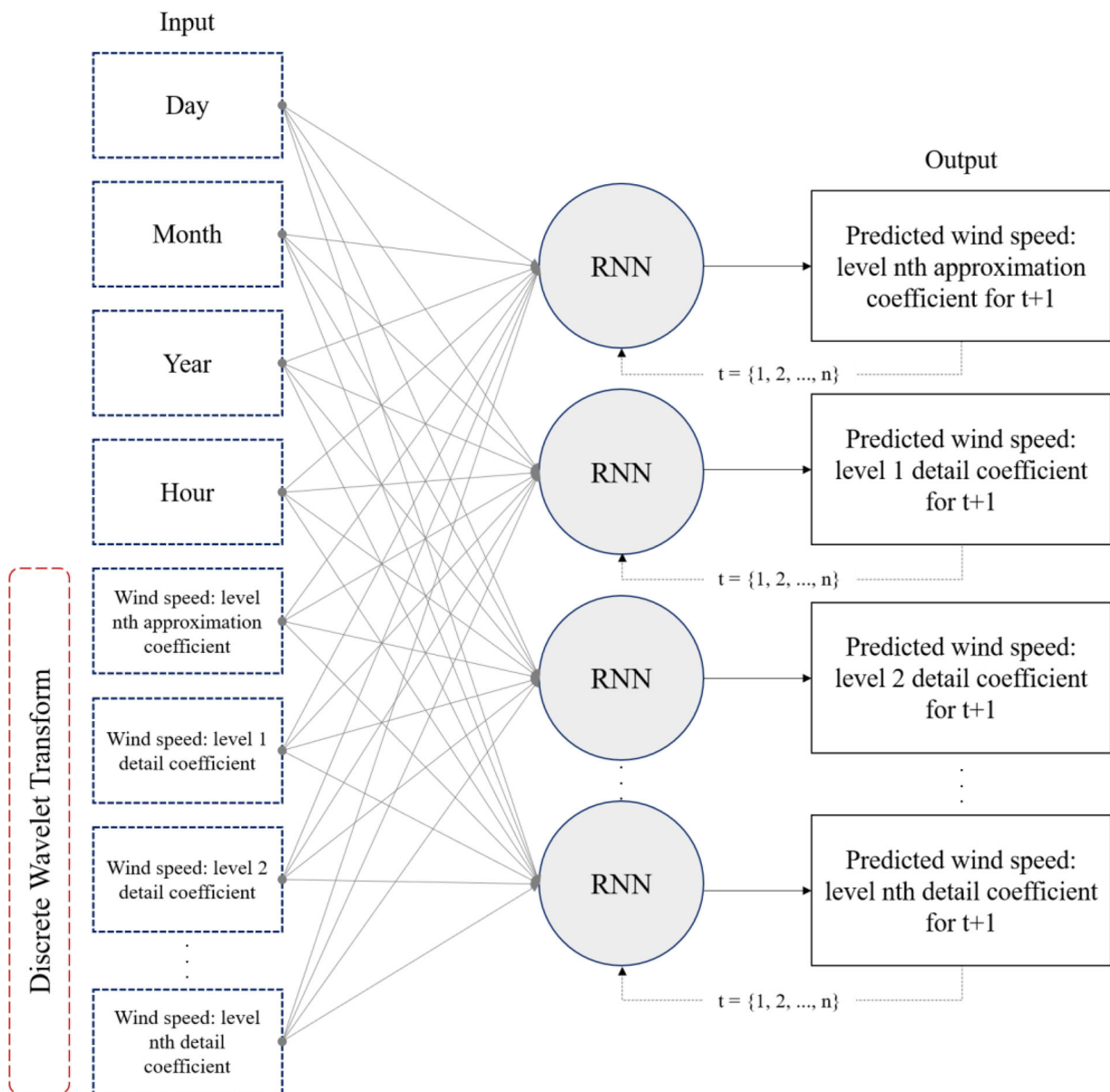


**Figure 14.** Flowchart of the procedure using RNN + Wavelet decomposition.

**Table 3.** Weibull shape factor and Weibull scale parameter.

| Sites     | Anemometer height [m] | k = the Weibull shape factor [unitless] | c = the Weibull scale parameter [m/s] |
|-----------|-----------------------|---|---------------------------------------|
| Esplanada | 100.0                 | 3.590                                   | 3.134                                 |
|           | 120.0                 | 3.806                                   | 3.340                                 |
|           | 150.0                 | 3.988                                   | 3.587                                 |
| Mucugê    | 100.0                 | 3.642                                   | 5.329                                 |
|           | 120.0                 | 3.653                                   | 5.280                                 |
|           | 150.0                 | 3.627                                   | 5.355                                 |
| Mucuri    | 100.0                 | 2.947                                   | 5.312                                 |
|           | 120.0                 | 3.132                                   | 5.420                                 |
|           | 150.0                 | 3.374                                   | 5.581                                 |

The best ANN configurations for Mucuri, Esplanada, and Mucugê are shown in Tables 4 and 5. This distribution of neurons was obtained empirically by testing different values and varying the amount of

processing neurons and learning rate until obtaining the best results.

The neural network configurations shown in the previous tables detected as the most efficient in

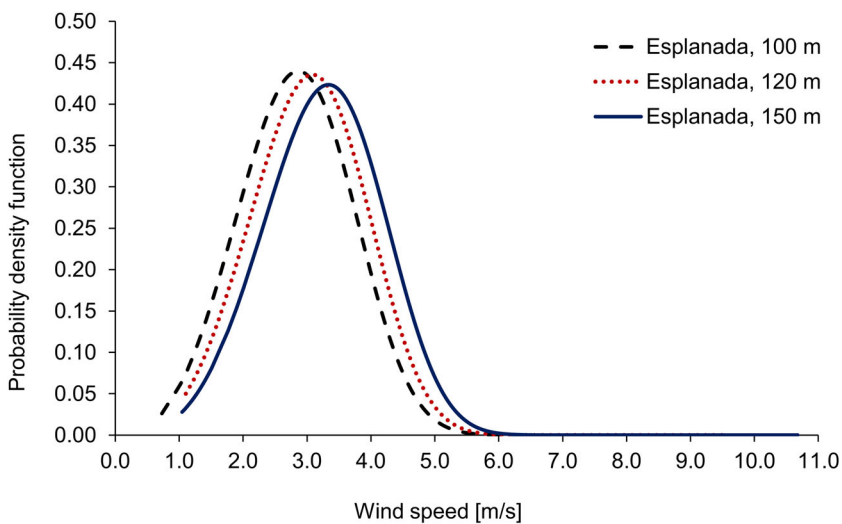


**Figure 15.** Weibull distribution density versus wind speed. Site: Esplanada.

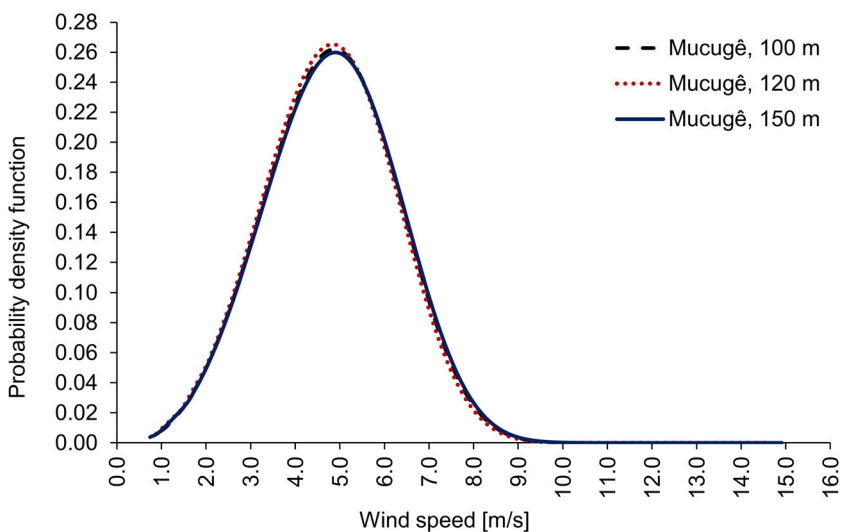


**Figure 16.** Weibull distribution density versus wind speed. Site: Mucugê.

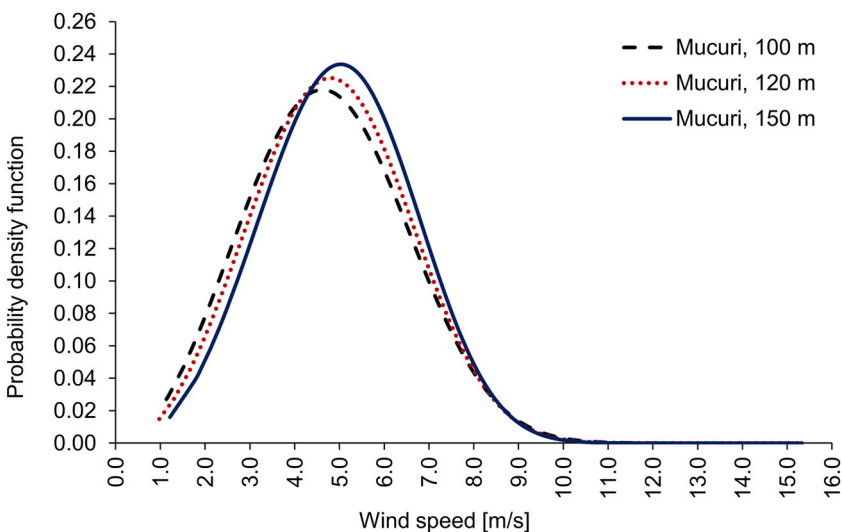


**Figure 17.** Weibull distribution density versus wind speed. Site: Mucuri.

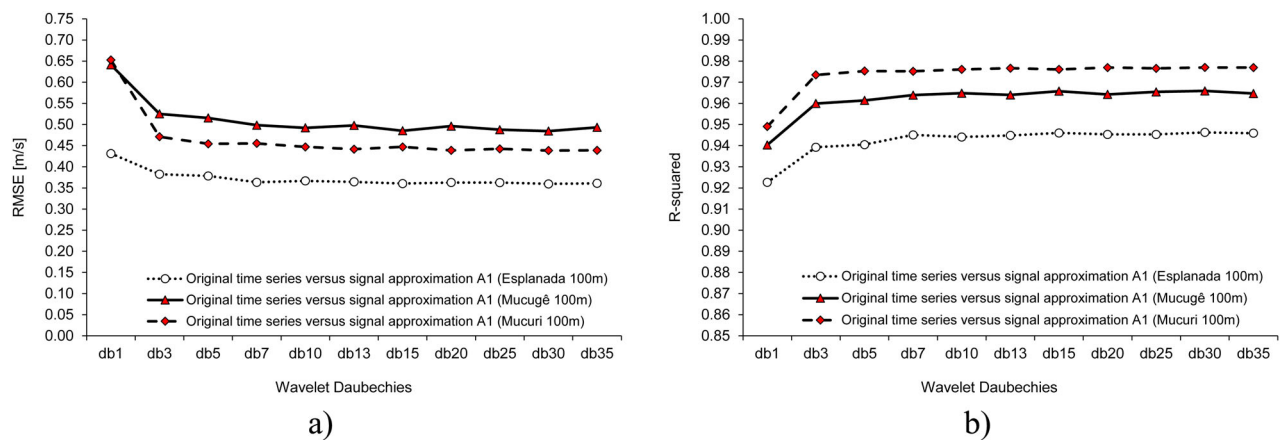


Figure 18. Wavelet Daubechies (db) decomposition. RMSE (a),  $R^2$  (b).

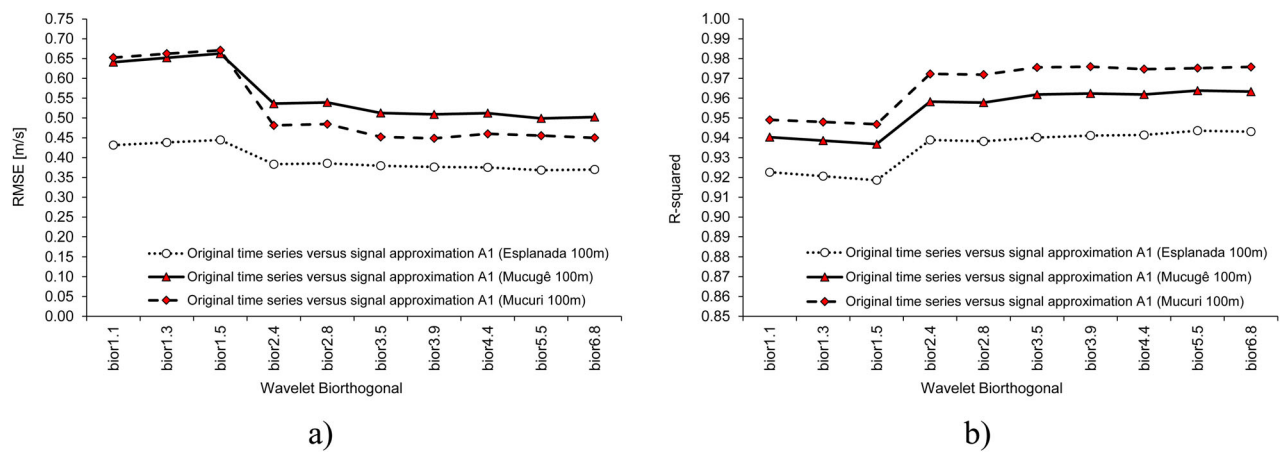


Figure 19. Wavelet Biorthogonal (bior) decomposition. RMSE (a),  $R^2$  (b).

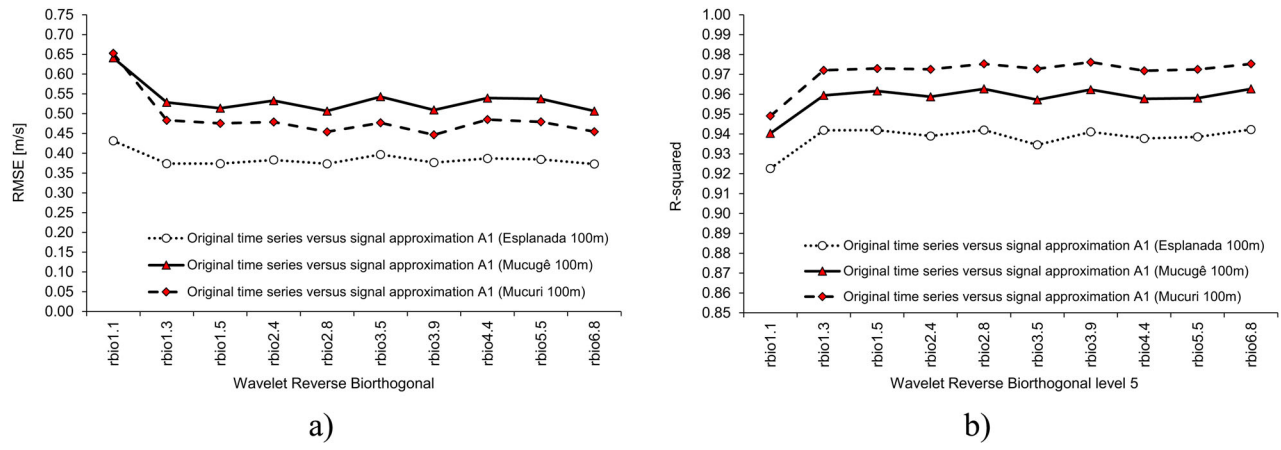
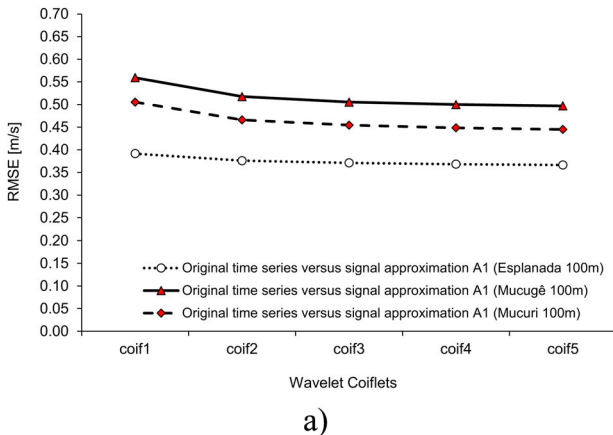


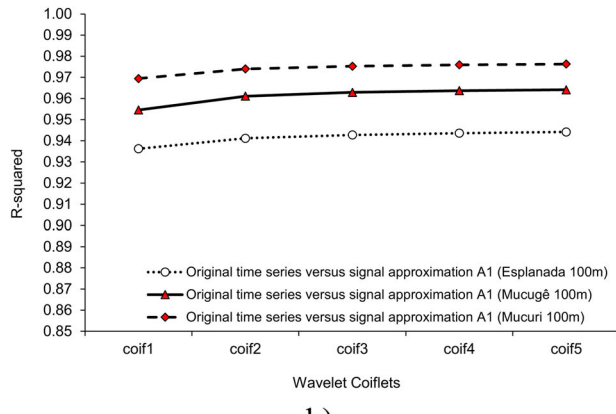
Figure 20. Wavelet Reverse biorthogonal (rbio) decomposition. RMSE (a),  $R^2$  (b).

precision and accuracy were used to predict the wind speed from 1 h to 6 h (nowcasting) in Mucuri, Esplanada, and Mucugê at all the heights tested. Tables 6 and 7 show the evaluation metrics of the prediction results (1 h, 3 h, and 6 h ahead) obtained by the MLP model, and RNN + Wavelet decomposition (hybrid model), respectively.

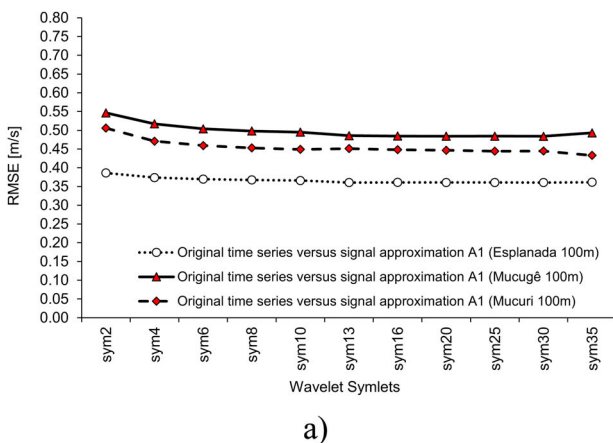
In Tables 6 and 7 it can be observed that, as the wind speed forecasting load increases, there is a reduction in the quality of the predicted data during ANN forecasting so that the higher the forecasting time, the greater the associated error measured by RMSE, and this is following what the literature describes [23–26]. It is observed that the statistical



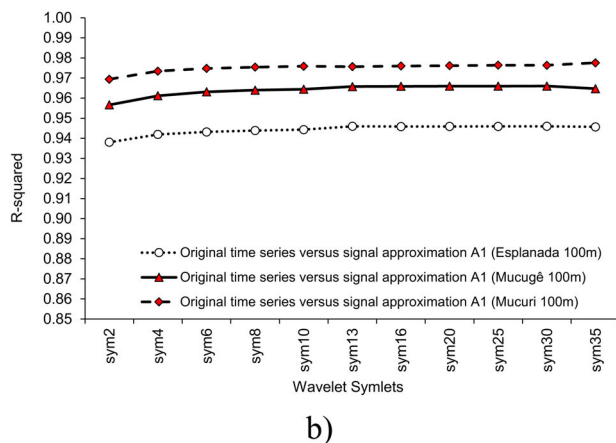
a)

**Figure 21.** Wavelet Coiflets (coif) decomposition. RMSE (a),  $R^2$  (b).

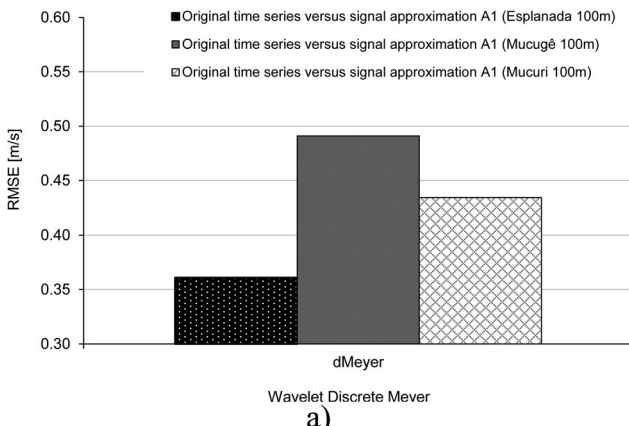
b)



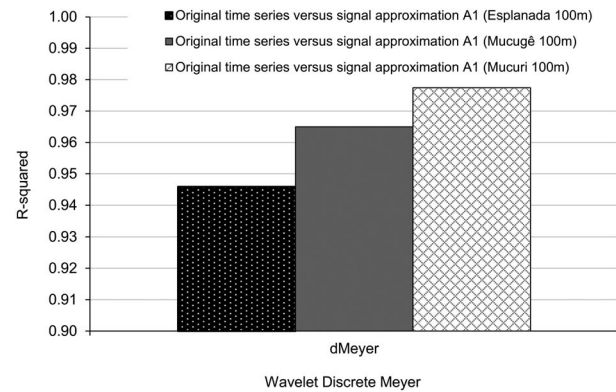
a)

**Figure 22.** Wavelet Symlets (sym) decomposition. RMSE (a),  $R^2$  (b).

b)



a)

**Figure 23.** Wavelet discrete Meyer (dMeyer) decomposition. RMSE (a),  $R^2$  (b).

b)

results reported in this study show that the computational model is applicable in any site and any anemometer height, given the low variability of such results. In short, it is very important to analyze the neural network architectures that will be applied in the prediction tests, because they adapt to the anemometric data set (or time series).

When a critical analysis is made on the statistical meters calculated and recorded in this work, we understand that the application of artificial intelligence through supervised machine learning along with the Wavelet decomposition (e.g. hybrid computational method) is a viable technique to predict the wind speed and, therefore, the wind energy generation,

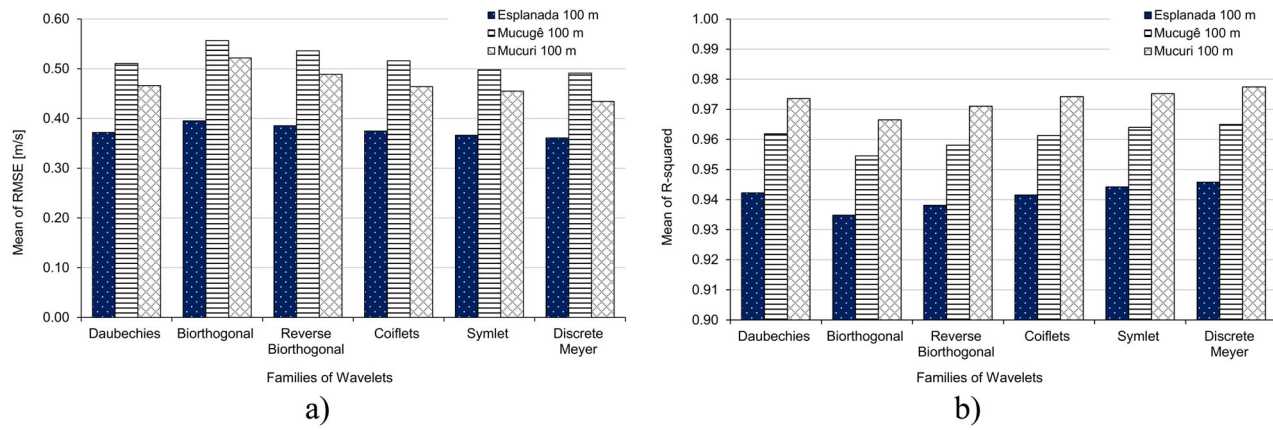


**Figure 24.** Wavelet families' statistical results. RMSE (a),  $R^2$  (b).

**Table 4.** The best ANN (MLP) configuration.

| Site        | Anemometer height<br>The best ANN configuration |         |         |
|-------------|---|---------|---------|
|             | 150.0 m   | 120.0 m | 100.0 m |
| Esplanada   | 7   | 7       | 7       |
| Mucugé      | 6   | 7       | 3       |
| Mucuri [16] | 1   | 6       | 6       |

| Site      | The best learning rate |         |         |
|-----------|------------------------|---------|---------|
|           | 150.0 m                | 120.0 m | 100.0 m |
| Esplanada | 0.001                  | 0.300   | 0.001   |
| Mucugé    | 0.300                  | 0.900   | 0.300   |
| Mucuri    | 0.900                  | 0.300   | 0.010   |

**Table 5.** The best ANN (RNN + Wavelet decomposition) configuration.

| Site      | Anemometer height<br>The best ANN configuration |         |         |
|-----------|---|---------|---------|
|           | 150.0 m   | 120.0 m | 100.0 m |
| Esplanada | 5   | 6       | 5       |
| Mucugé    | 3   | 3       | 5       |
| Mucuri    | 6   | 6       | 1       |

| Site      | The best learning rate |         |         |
|-----------|------------------------|---------|---------|
|           | 150.0 m                | 120.0 m | 100.0 m |
| Esplanada | 0.010                  | 0.010   | 0.010   |
| Mucugé    | 0.900                  | 0.900   | 0.010   |
| Mucuri    | 0.900                  | 0.010   | 0.010   |

**Table 6.** The contrast between RMSE, Pearson, and Fac2 values depending on site, and anemometer height. ANN: MLP.

| Site / Anemometer height                    | Time horizon | mean RMSE [m/s] | mean Pearson correlation coefficient | mean Percentage of the data of a factor of two (Fac2) |
|---|--------------|-----------------|--------------------------------------|---|
| Esplanada (100.0 m, 120.0 m, and 150.0 m)   | 1 h          | 1.020           | 0.784                                | 98.79%  |
| Mucugé (100.0 m, 120.0 m, and 150.0 m)      |              | 1.384           | 0.879                                | 98.79%  |
| Mucuri (100.0 m, 120.0 m, and 150.0 m) [16] |              | 0.942           | 0.943                                | 100%  |
| Esplanada (100.0 m, 120.0 m, and 150.0 m)   | 3 h          | 1.424           | 0.522                                | 98.43%  |
| Mucugé (100.0 m, 120.0 m, and 150.0 m)      |              | 2.154           | 0.673                                | 95.81%  |
| Mucuri (100.0 m, 120.0 m, and 150.0 m) [16] |              | 1.729           | 0.818                                | 99.65%  |
| Esplanada (100.0 m, 120.0 m, and 150.0 m)   | 6 h          | 1.765           | 0.258                                | 95.17%  |
| Mucugé (100.0 m, 120.0 m, and 150.0 m)      |              | 2.787           | 0.463                                | 90.07%  |
| Mucuri (100.0 m, 120.0 m, and 150.0 m) [16] |              | 2.902           | 0.512                                | 92.37%  |

mainly due to the low cost and low computational time. However, it's essential to carefully choose the architecture of the neural network (or topology) and its hyperparameters that best matches the wind power forecasting project, in addition to the need to make a quantitative and qualitative analysis of the anemometric

data that will feed the neural network, since these predictors directly impact the predicted results (in this case, the wind speed). Figures 25–27 describe the mean squared error (MSE). Given all the cases projected in the figures, 100% were more accurate when using computational intelligence + Wavelet decomposition (i.e.

**Table 7.** The contrast between RMSE, Pearson, and Fac2 values depending on site, and anemometer height. ANN: RNN + discrete Meyer Wavelet decomposition (dmey).

| Site / Anemometer height                  | Time horizon | mean RMSE [m/s] | mean Pearson correlation coefficient | mean Percentage of the data of a factor of two |
|---|--------------|-----------------|--------------------------------------|--|
| Esplanada (100.0 m, 120.0 m, and 150.0 m) | 1 h          | 0.814           | 0.832                                | 100%   |
| Mucugê (100.0 m, 120.0 m, and 150.0 m)    |              | 0.821           | 0.962                                | 99.48%   |
| Mucuri (100.0 m, 120.0 m, and 150.0 m)    |              | 0.870           | 0.951                                | 100%   |
| Esplanada (100.0 m, 120.0 m, and 150.0 m) | 3 h          | 1.272           | 0.662                                | 97.73%   |
| Mucugê (100.0 m, 120.0 m, and 150.0 m)    |              | 1.581           | 0.856                                | 98.43%   |
| Mucuri (100.0 m, 120.0 m, and 150.0 m)    |              | 1.501           | 0.853                                | 99.13%   |
| Esplanada (100.0 m, 120.0 m, and 150.0 m) | 6 h          | 1.597           | 0.487                                | 97.16%   |
| Mucugê (100.0 m, 120.0 m, and 150.0 m)    |              | 2.259           | 0.717                                | 97.16%   |
| Mucuri (100.0 m, 120.0 m, and 150.0 m)    |              | 1.713           | 0.815                                | 97.87%   |

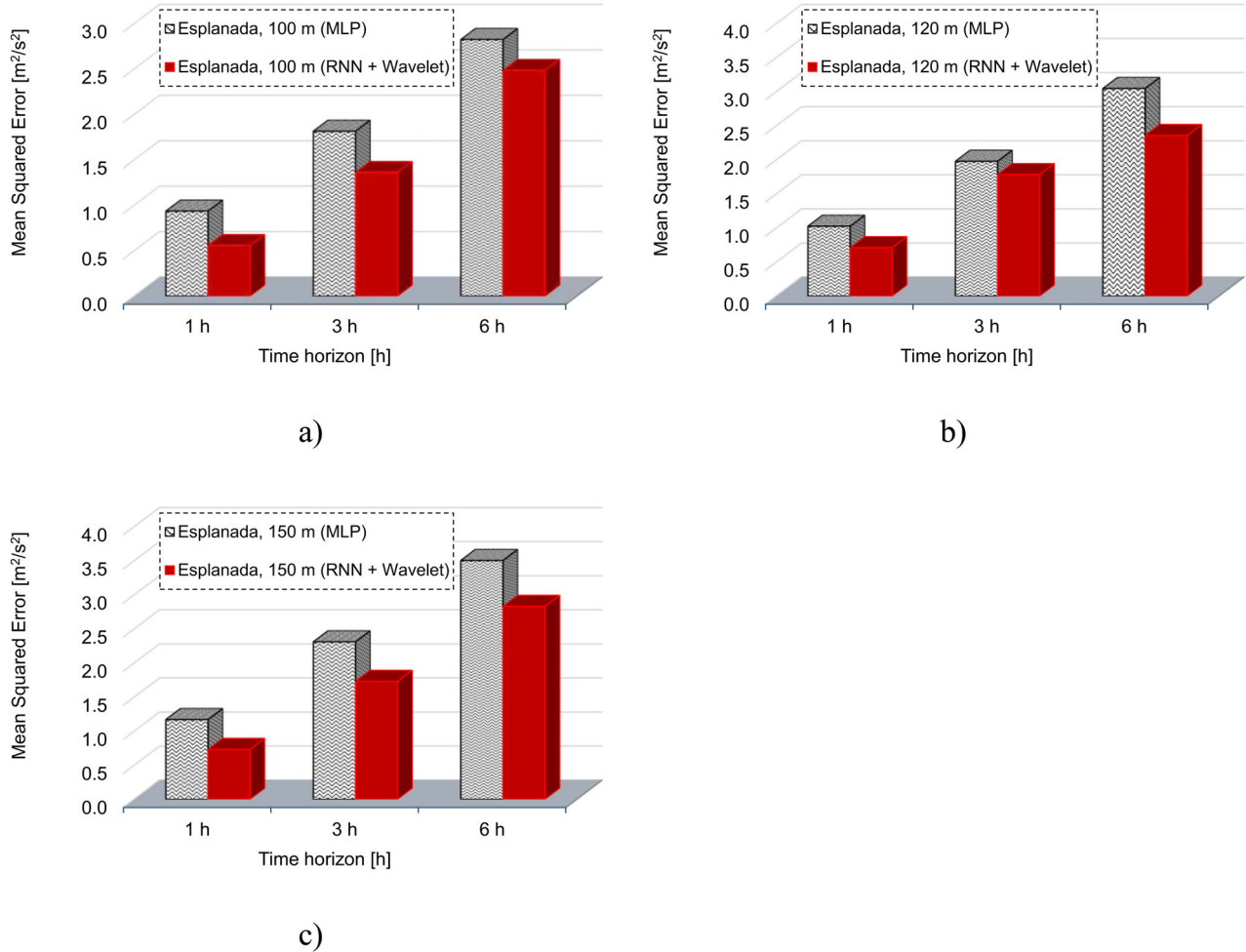


**Figure 25.** MSE results for Esplanada, 100.0 m (a), 120.0 m (b), and 150.0 m (c).

RNN + dmey). Which justifies the use of energy in this scientific investigation. The Wavelet decomposition eliminates noisy components from the wind time series, and the supervised machine learning by ANN provides a multistep forecast on the sub-signals obtained from the decomposition technique.

Figure 28 shows the comparison of the MSE statistical descriptive measure comparing the three sites and the three anemometers heights applied in this work.

Figures 29–31 show the best prediction results (nowcasting) using hybrid computational model for the sites Esplanada, Mucugê, and Mucuri (computational model: RNN + dmey). In the figures: a) is the results of the 6-step forecasting of the wind speed series, and b) and c) comparison data of Fac2.

Papers such as those developed by [27–30] highlight the relevance of studies on ANN applied to wind time series with the ultimate goal of improving wind field forecasting technologies and then the short-term

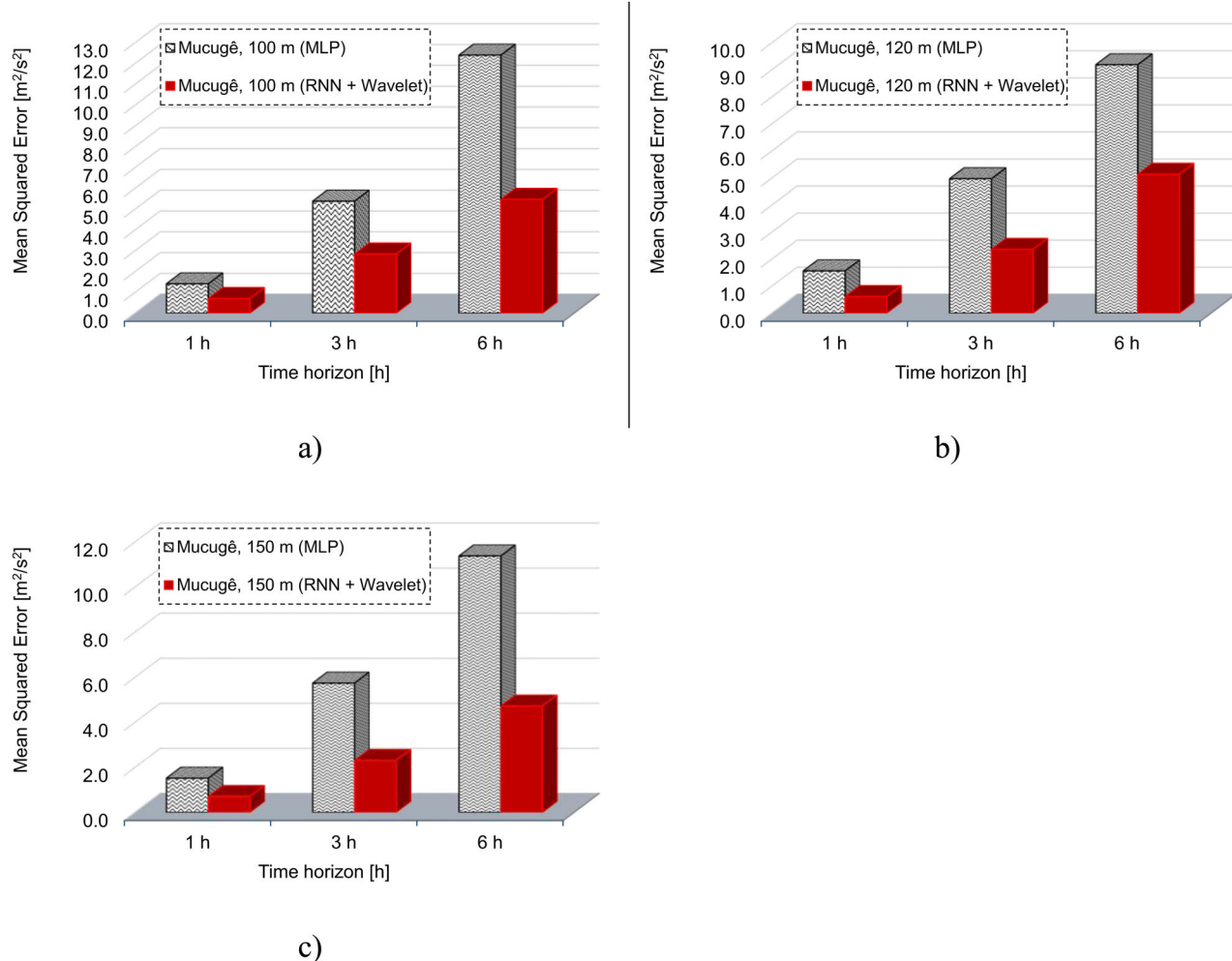


**Figure 26.** MSE results for Mucugê, 100.0 m (a), 120.0 m (b), and 150.0 m (c).

forecasting for energy. This directly helps the operators of the electrical matrix of the region in question and helps other regions to develop sustainably, especially using wind energy. This paper shows the short-term wind speed forecasting in the humid tropical region of Bahia, Brazil, applying the Wavelet decomposition and the ANN technique to the hourly time series representative of the site. It uses an approach to train the model for the next hour forecasting, then recursively inferring the forecasting for the following hours. This kind of method has low computational costs when compared with numerical modeling. The results achieved and recorded in this research are important for improving knowledge about the application of the Wavelet decomposition in the time series of the wind through the different families. Different families provide different relationships between how compact the basis function is localized in space and how smooth they're.

The dmey Wavelet provides the best results among all the included 48 mother Wavelet functions. These

results agree with the results published by empirical evidence in the literature. Zucatelli et al. [17] showed a comparison of the mean squared error and R-squared to MLP, RNN, and RNN + Wavelet decomposition. The Wavelet families applied to wind speed data decomposition were bior3.9 level 3, coif5 level 3, db7 level 3, db8 level 5, db9 level 7, dmey level 3 and sym7 level 3. The work presents that the RNN + dmey Wavelet decomposition has the best result. Multi-step prediction intervals are 1 h to 12 h ahead and the site is in Brazil. Already in Liu et al. [31] is showed that discrete Meyer Wavelet provides the best results among all the included 17 mother Wavelet functions. These mother Wavelet functions include the haar; the db4, db6 and db10; the coif1, coif2, coif3, coif4 and coif5; the sym2, sym3, sym4, sym5, sym6, sym7 and sym8 and the dmey. Multi-step prediction intervals are 1 h to 7 h ahead and the sites are in China. Then, the results published empirically in the literature showed that the discrete Meyer is the most efficient when compared to the other Wavelet families.

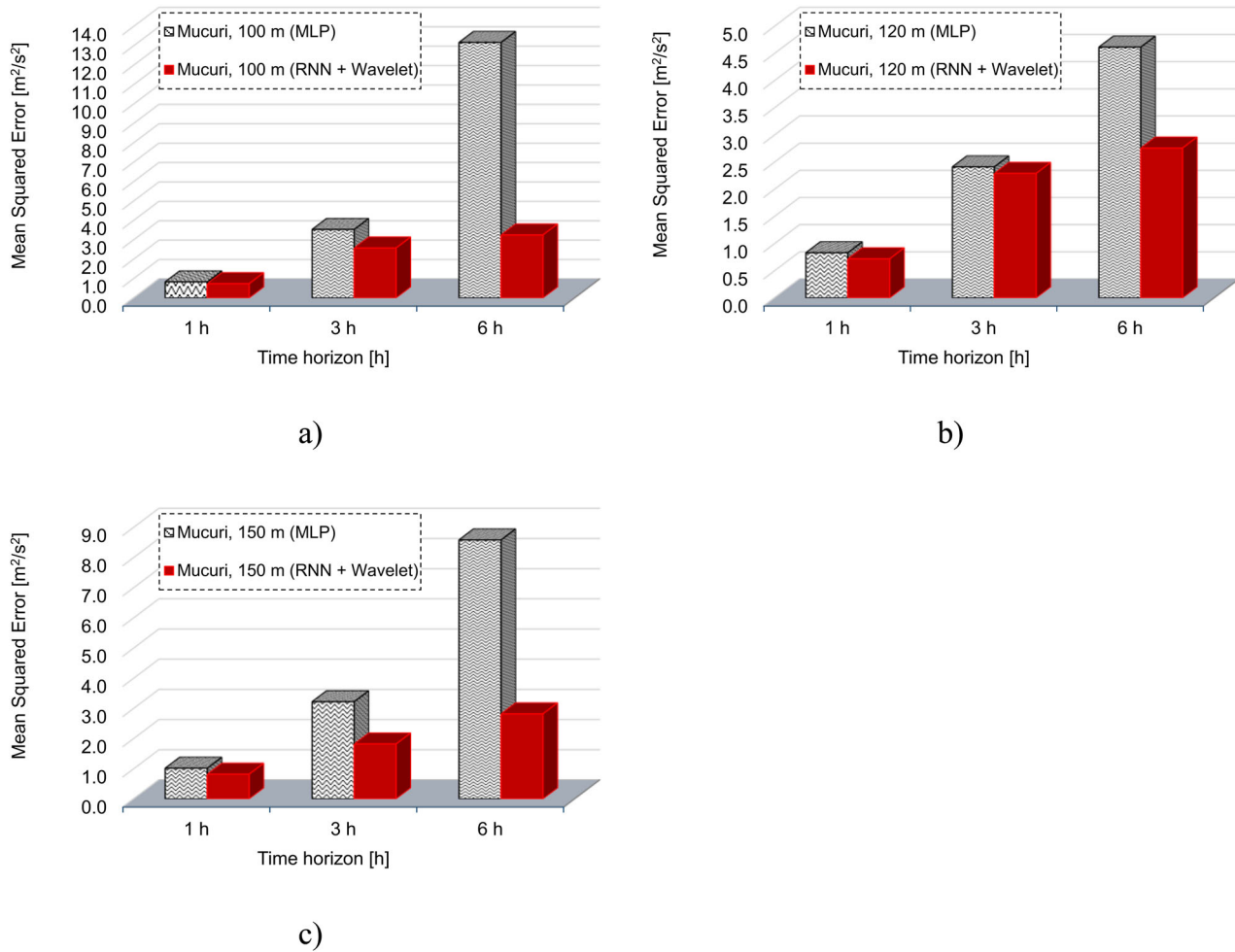


**Figure 27.** MSE results for Mucuri, 100.0 m (a), 120.0 m (b), and 150.0 m (c).

The wind speed forecasting accurately in a time horizon of 1 h to 6 h ahead (nowcasting) contributes to the hourly commercialization of wind power, either in Brazil or in another country. It should be emphasized that the computational cost due to the application of computational intelligence by machine learning in studies such as those carried out in this work increases as the expected workload increases, but it is even lower when compared to the cost of mathematical modeling and numerical simulation for wind prediction using atmospheric models, such as weather research and forecasting (WRF). The WRF is a great example of a numerical model of weather forecasts used both for the operation of meteorological centers and for atmospheric research. The most outstanding features of the WRF are the multiple dynamic cores, a variable 3D data assimilation system, and a software structure that allows computational parallelism, as well as the extensibility of the system. In this way, the computational time resulting from the use of numerical forecasting models (Prediktor, Previento, LocalPred, eWind, and WRF, for example)

with refined simulation grids for a short to the medium-term horizon in microscale spatial resolution, it ends up, many times, not justifying the cost-benefit. These models are well used for forecasting with mesoscale spatial resolution and long-term horizon. In contrast, the persistence method and statistical methods (Autoregressive Model, Autoregressive Moving Average, and Autoregressive Integrated Moving Average - ARIMA, for example) in most studies are applied to forecast up to 1 h ahead, as variability and fluctuations observations of the observed data end up reducing the accuracy of the forecast. Thus, the forecast for wind energy in the short-term can be improved using this hybrid model to improve the quality of wind energy 1 h to 6 h ahead supplied to the power grid.

#### 4. Conclusion and future works

The objective of this work was to present the short-term wind speed prediction 6 h ahead (or nowcasting) for three sites in the state of Bahia (Esplanada,

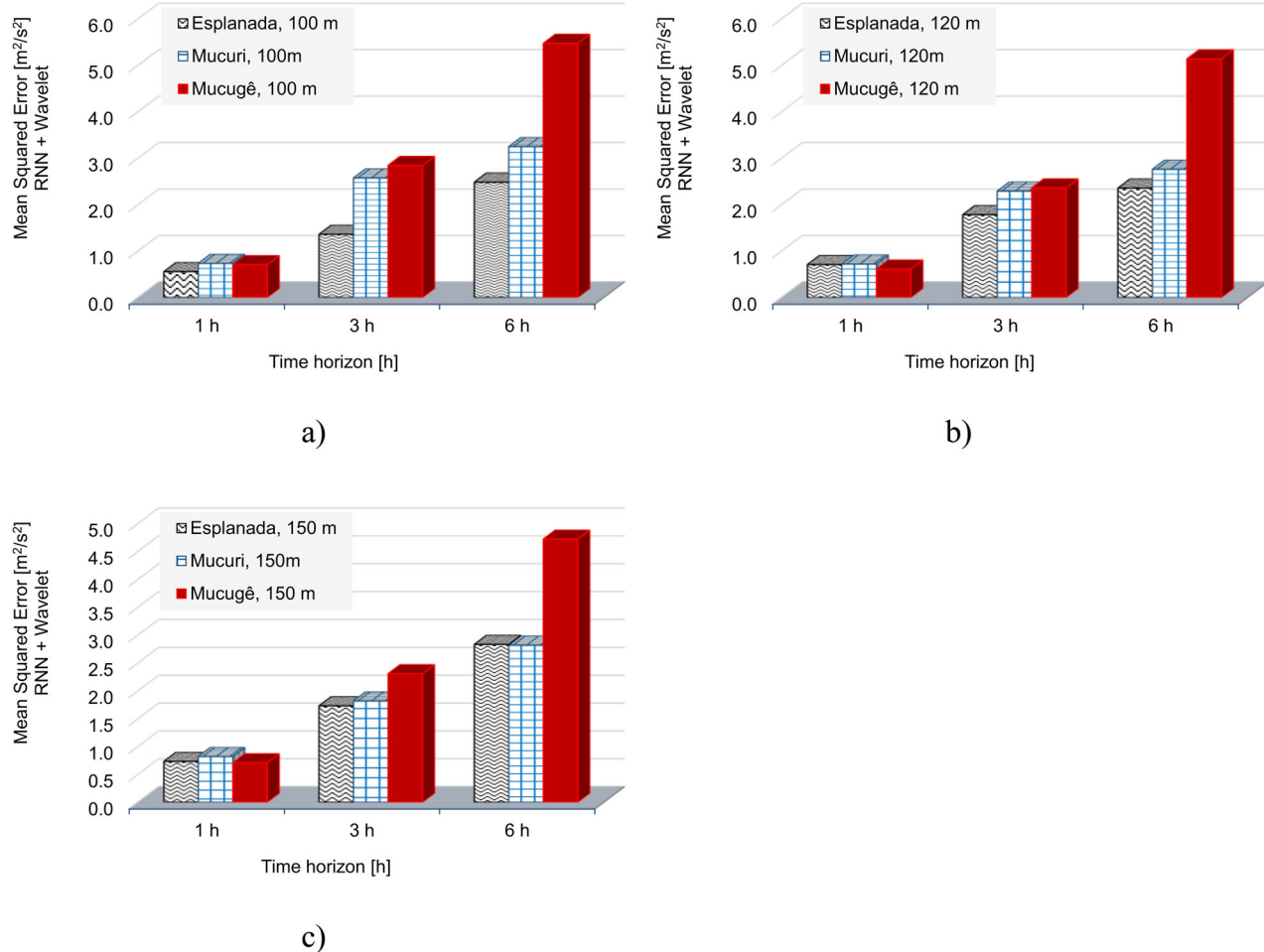
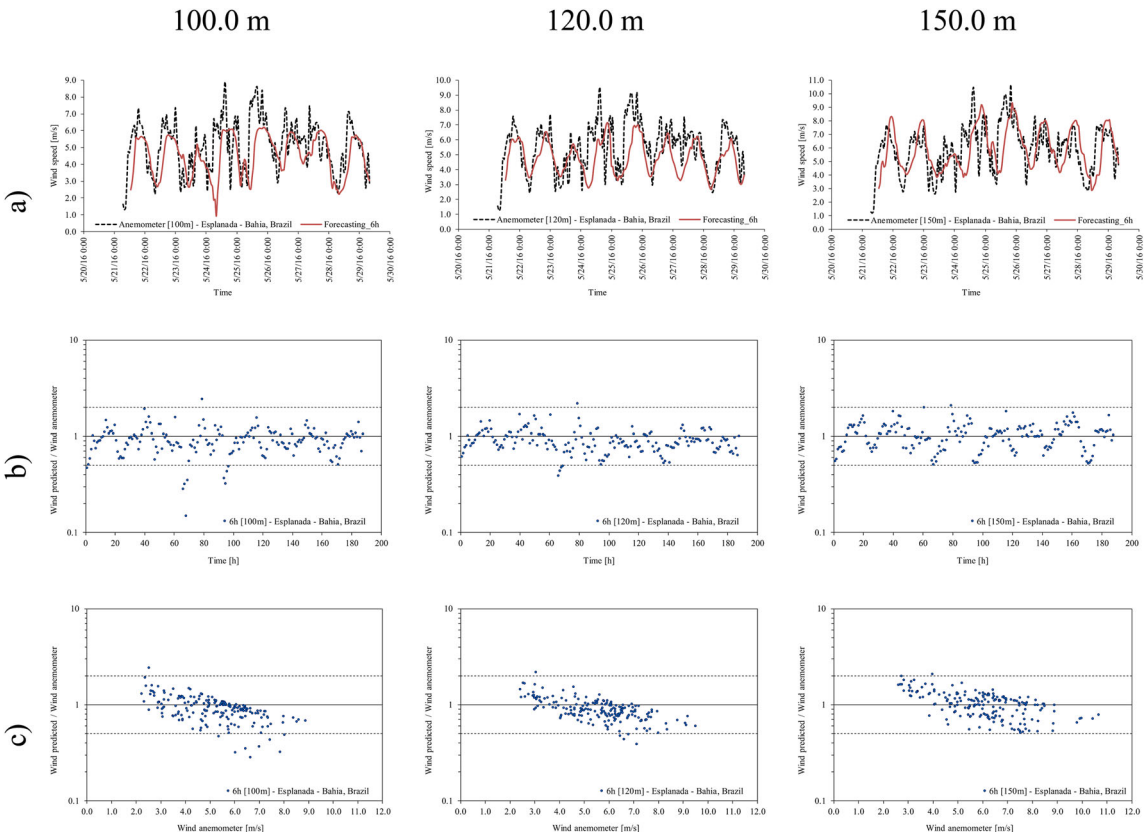


Figure 28. MSE results (RNN + dmey) for Esplanada, Mucuri, and Mucugê at 100.0 m (a), 120.0 m (b), and 150.0 m (c).

Mucugê, and Mucuri), which is one of the most important Brazilian states in terms of renewable energy production. For this, it was applied the computational intelligence by ANN technique, which was trained, validated, and tested using data collected in anemometric towers installed at 100.0 m, 120.0 m, and 150.0 m height (average hourly values of the wind speed, wind direction, air temperature, air humidity, and air pressure). The wind energy is the fastest-growing type of renewable energy in Brazil and these results are presented as a novelty, since other works that used this computational model to predict wind speed for 1 h to 6 h (nowcasting) in Bahia state, Brazil, especially in the Esplanada, Mucugê, and Mucuri cities, were not found in other scientific research published, particularly in positions where the hub of the wind turbine are usually positioned, such as the anemometric heights of this study, which were 100.0 m, 120.0 m, and 150.0 m. The application of the technique of ANN and Wavelet decomposition to predict the wind speed at different heights and sites was

adequate when interpreting the statistical results. Especially, it can be pointed out that the 6 h forecast presented good results (by RNN + Wavelet discrete Meyer) with low computational costs, helping wind farm operators in decision-making processes, as ONS in Brazil. Then, the results showed that the application of the hybrid machine learning algorithm (supervised machine learning by RNN + Wavelet decomposition, using discrete Meyer) to predict the wind speed at different Bahia's sites and higher heights presented good accuracy, attesting its ability to be used as a powerful tool to ONS to improve the usage and integration of the wind energy into the national electrical grid. Globally, wind power has lessened the burden on conventional fossil fuel-based power generation. Wind resource assessment for wind farms aids accurate forecasting and analyzing the nature of ramp events, for example. An important outcome of this study is that machine learning algorithms could be successfully used to wind forecasting before the establishment of wind plants in a potential



**Figure 29.** Wind speed prediction 6 h ahead (nowcasting), in Esplanada. Dataset: 05/21/2016 at 7:00 a.m. until 05/29/2016 at 8:00 a.m.

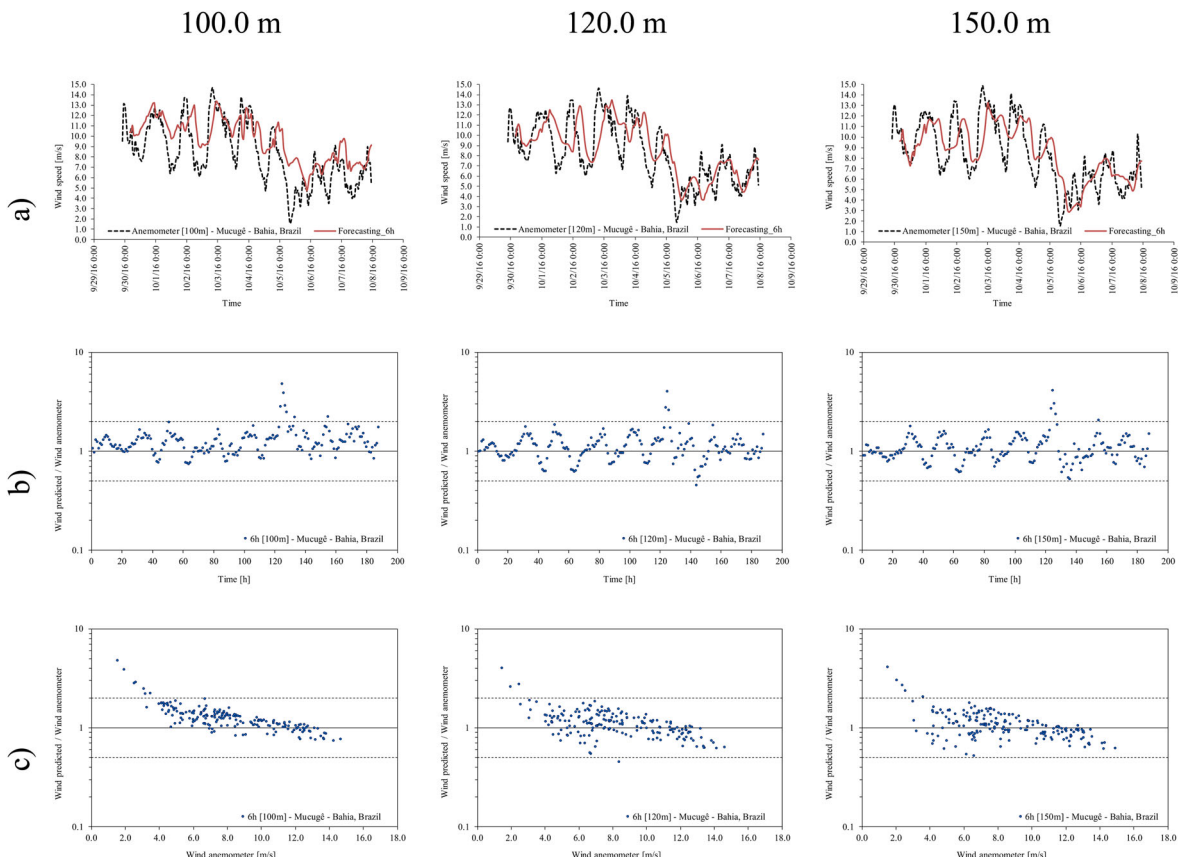


**Figure 30.** Wind speed prediction 6 h ahead (nowcasting), in Mucugê. Dataset: 09/29/2016 at 10:00 p.m. until 10/07/2016 at 11:00 p.m.

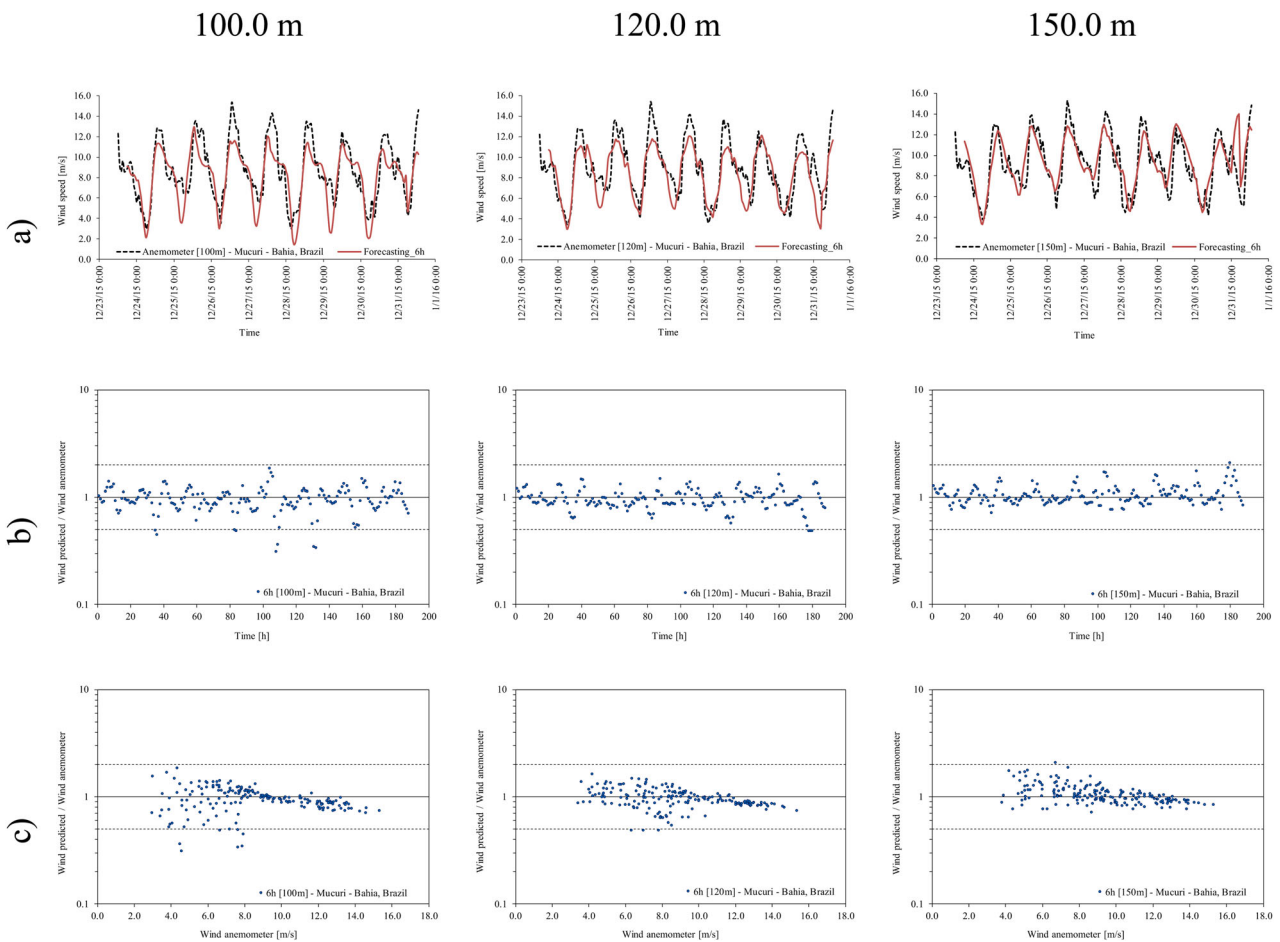


**Figure 31.** Wind speed prediction 6 h ahead (nowcasting), in Mucuri. Dataset: 12/23/2015 at 12:00 p.m. until 12/31/2015 at 1:00 p.m.

location. We leave it as a suggestion for future work on this research: to use the Mucugê, Esplanada, Mucuri, and other observational data collected in different heights in Brazil and Uruguay to perform the forecast of the wind power. The next papers can apply computational intelligence by supervised machine learning aiming the medium and long-term wind speed forecasting applying long short-term memory (LSTM), gated recurrent units (GRU), convolutional neural networks (CNN), Wavelet neural network (WNN) and to compare these results with the output produced by numerical weather prediction (NWP) using mathematical models. Wind power and wind ramp forecasting using computational intelligence, and self-organizing map (SOM) in wind speed forecasting are also a great subject of research to the electric power sector.

## Acknowledgements

We thank Manufacturing and Technology Integrated Campus – SENAI CIMATEC, Salvador, Bahia, Brazil, for their computational support.

## Disclosure statement

We wish to confirm that there are no known conflicts of interest associated with this publication and there has been no significant financial support for this work that could have influenced its outcome.

## ORCID

- Pedro Junior Zucatelli <http://orcid.org/0000-0002-6744-5376>
- Erick Giovani Sperandio Nascimento <http://orcid.org/0000-0003-2219-0290>
- Alex Álisson Bandeira Santos <http://orcid.org/0000-0001-9935-4084>
- Davidson Martins Moreira <http://orcid.org/0000-0002-0902-5218>

## References

- [1] W. Y. Y. Cheng, Y. Liu, A. J. Bourgeois, Y. Wu and S. E. Haupt, "Short-term wind forecast of a data assimilation/weather forecasting system with wind turbine anemometer measurement assimilation," *Renewable Energy*, vol. 107, pp. 340–351, July 2017. DOI: [10.1016/j.renene.2017.02.014](https://doi.org/10.1016/j.renene.2017.02.014).

- [2] P. Jiang, Y. Wang and J. Wang, "Short-term wind speed forecasting using a hybrid model," *Energy*, vol. 119, pp. 561–577, Jan. 2017. DOI: [10.1016/j.energy.2016.10.040](https://doi.org/10.1016/j.energy.2016.10.040).
- [3] C. Li, Z. Xiao, X. Xia, W. Zou and C. Zhang, "A hybrid model based on synchronous optimisation for multi-step short-term wind speed forecasting," *Appl. Energy*, vol. 215, pp. 131–144, Apr. 2018. DOI: [10.1016/j.apenergy.2018.01.094](https://doi.org/10.1016/j.apenergy.2018.01.094).
- [4] C. Huang, F. Li and Z. Jin, "Maximum power point tracking strategy for large-scale wind generation systems considering wind turbine dynamics," *IEEE Trans. Ind. Electron.*, vol. 62, no. 4, pp. 2530–2539, Apr. 2015. DOI: [10.1109/TIE.2015.2395384](https://doi.org/10.1109/TIE.2015.2395384).
- [5] C. S. Tian, Y. Hao and J. M. Hu, "A novel wind speed forecasting system based on hybrid data pre-processing and multi-objective optimization," *Appl. Energy*, vol. 231, pp. 301–319, Dec. 2018. DOI: [10.1016/j.apenergy.2018.09.012](https://doi.org/10.1016/j.apenergy.2018.09.012).
- [6] C. Li, Z. J. Zhu, H. F. Yang and R. R. Li, "An innovative hybrid system for wind speed forecasting based on fuzzy preprocessing scheme and multi-objective optimization," *Energy*, vol. 174, pp. 1219–1237, May 2019. DOI: [10.1016/j.energy.2019.02.194](https://doi.org/10.1016/j.energy.2019.02.194).
- [7] Y. F. Li, H. P. Shi, F. Z. Han, Z. Duan and H. Liu, "Smart wind speed forecasting approach using various boosting algorithm, big multi-step forecasting strategy," *Renewable Energy*, vol. 135, pp. 540–553, May 2019. DOI: [10.1016/j.renene.2018.12.035](https://doi.org/10.1016/j.renene.2018.12.035).
- [8] Y. Wang, H. B. Wang, D. Srinivasan and Q. Hu, "Robust functional regression for wind speed forecasting based on Sparse Bayesian learning," *Renewable Energy*, vol. 132, pp. 43–60, Mar. 2019. DOI: [10.1016/j.renene.2018.07.083](https://doi.org/10.1016/j.renene.2018.07.083).
- [9] R. Kaja Bantha Navas, S. Prakash and T. Sasipraba, "Artificial neural network based computing model for wind speed prediction: A case study of Coimbatore, Tamil Nadu, India," *Physica A: Statistical Mechanics Its Appl.*, vol. 542, pp. 123383, Mar. 2020. DOI: [10.1016/j.physa.2019.123383](https://doi.org/10.1016/j.physa.2019.123383).
- [10] W. Tong, "Chapter 1: Fundamentals of wind energy," in *Wind Power Generation and Wind Turbine Design*, vol. 44, USA: WIT Press, 2010, pp. 3–46. Available: <https://www.witpress.com/Secure/elibrary/papers/9781845642051/9781845642051001FU1.pdf>. DOI: [10.2495/978-1-84564-205-1/01](https://doi.org/10.2495/978-1-84564-205-1/01).
- [11] I. Kuikka, "Wind nowcasting: Optimizing runway in use," Technical report, Systems Analysis Laboratory, Helsinki University of Technology, 2009. Available: <https://www.mdpi.com/1996-1073/12/16/3050/pdf>
- [12] H. S. Dhiman, D. Deb and V. E. Balas, "Chapter 6 - Hybrid machine intelligent wind speed forecasting models", in *Supervised Machine Learning in Wind Forecasting and Ramp Event Prediction*, USA: Academic Press, 2020, pp. 75–99. DOI: [10.1016/B978-0-12-821353-7.00017-X](https://doi.org/10.1016/B978-0-12-821353-7.00017-X)
- [13] D. B. Alencar, C. M. Affonso, R. C. L. Oliveira, J. L. M. Rodriguez, J. C. Leite and J. C. R. Filho, "Different models for forecasting wind power generation: Case study," *Energies*, vol. 10, no. 12, pp. 1976, 2017. DOI: [10.3390/en10121976](https://doi.org/10.3390/en10121976).
- [14] P. J. Zucatelli, et al., "Short-term wind speed forecasting in Uruguay using computational intelligence," *Heliyon*, vol. 5, no. 5, pp. e01664, May 2019. DOI: [10.1016/j.heliyon.2019.e01664](https://doi.org/10.1016/j.heliyon.2019.e01664).
- [15] P. J. Zucatelli, E. G. S. Nascimento, A. A. B. Santos, A. M. G. Arce and D. M. Moreira, *Study of the Wind Speed Forecasting Applying Computational Intelligence*. Rijeka: IntechOpen, 2019. DOI: [10.5772/intechopen.89758](https://doi.org/10.5772/intechopen.89758). Available: <https://www.intechopen.com/online-first/study-of-the-wind-speed-forecasting-applying-computational-intelligence>.
- [16] P. J. Zucatelli, et al., "Short-term wind speed forecasting using computational intelligence in Bahia, Brazil," In Proceedings of the Air Pollution Conference Brazil and 4th CMAS South America, 2019. Extended Abstract, Belo Horizonte, 2019. Available: <https://com.us14.list-manage.com/subscribe?u=2498509b374e6e196b427a2c4&id=162bf02c3d>.
- [17] P. J. Zucatelli, E. G. S. Nascimento, L. R. Campos, A. A. B. Santos and D. M. Moreira, "Short-term wind speed forecasting in tropical region using wavelets and artificial intelligence," In Proceedings of the International Symposium on Innovation and Technology (SIINTEC), 2019, pp. 365–372. DOI: [10.5151/siintec2019-46](https://doi.org/10.5151/siintec2019-46). Available: [https://www.proceedings.blucher.com.br/article-details/previo-da-velocidade-do-vento-a-curto-prazo-em-regiao-tropical-utilizando-Wavelets-e-inteligencia-artificial-33286](https://www.proceedings.blucher.com.br/article-details/previso-da-velocidade-do-vento-a-curto-prazo-em-regiao-tropical-utilizando-Wavelets-e-inteligencia-artificial-33286).
- [18] P. J. Zucatelli, E. G. S. Nascimento, A. M. G. Arce and D. M. Moreira, "Short-range wind speed predictions in subtropical region using artificial intelligence," *J. Systemics, Cybern. Informatics*, vol. 17, no. 4, pp. 1–8, 2019. Available: <http://www.iisci.org/journal/sci/Abstracts.asp?var=&previous=ISS1904>.
- [19] ABEEolica. 2020. Infowind Brazil Update 16 2020 - Jun, 15. Available: [http://abeeolica.org.br/wp-content/uploads/2020/06/InfoventoPT\\_16.pdf](http://abeeolica.org.br/wp-content/uploads/2020/06/InfoventoPT_16.pdf)
- [20] J. L. Paixão, et al., "Wind generation forecasting of short and very short duration using Neuro-Fuzzy Networks: A case study," 7th International Conference on Modern Power Systems (MPS 2017), IEEE, 2017. Available: <https://ieeexplore.ieee.org/document/7974446>. DOI: [10.1109/MPS.2017.7974446](https://doi.org/10.1109/MPS.2017.7974446).
- [21] S. Haykin, *Neural Networks: A Comprehensive Foundation*, 2nd ed. Hamilton, Ontario, Canada: Pearson Education Inc., 1999, pp. 823.
- [22] I. Daubechies, "Ten lectures on wavelets," CBMS-NSF Regional Conference Series in Applied Mathematics, SIAM, 1992. DOI: [10.1137/1.9781611970104](https://doi.org/10.1137/1.9781611970104).
- [23] A. Kusiak, H. Zheng and Z. Song, "Short-term prediction of wind farm power: A data mining approach," *IEEE Trans. Energy Conversion*, vol. 24, no. 1, pp. 125–136, Mar. 2009. DOI: [10.1109/TEC.2008.2006552](https://doi.org/10.1109/TEC.2008.2006552).
- [24] R. Blonbou, "Very short-term wind power forecasting with neural networks and adaptive Bayesian learning," *Renewable Energy*, vol. 36, no. 3, pp. 1118–1124, Mar. 2011. DOI: [10.1016/j.renene.2010.08.026](https://doi.org/10.1016/j.renene.2010.08.026).
- [25] A. Carpinone, M. Giorgio, R. Langella and A. Testa, "Markov chain modeling for very-short-term wind power forecasting," *Electric Power Syst. Res.*, vol. 122, pp. 152–158, May 2015. DOI: [10.1016/j.epsr.2014.12.025](https://doi.org/10.1016/j.epsr.2014.12.025).

- [26] Ü. B. Filik and T. Filik, "Wind speed prediction using artificial neural networks based on multiple local measurements in Eskisehir," *Energy Procedia*, vol. 107, pp. 264–269, Feb. 2017. DOI: [10.1016/j.egypro.2016.12.147](https://doi.org/10.1016/j.egypro.2016.12.147).
- [27] A. Brka, Y. M. Al-Abdely and G. Kothapalli, "Influence of neural network training parameters on short-term wind forecasting," *Int. J. Sustainable Energy*, vol. 35, no. 2, pp. 115–131, 2016. DOI: [10.1080/14786451.2013.873437](https://doi.org/10.1080/14786451.2013.873437).
- [28] D. Fang and J. Wang, "A novel application of artificial neural network for wind speed estimation," *Int. J. Sustainable Energy*, vol. 36, no. 5, pp. 415–429, 2017. DOI: [10.1080/14786451.2015.1026906](https://doi.org/10.1080/14786451.2015.1026906).
- [29] S. K. Jha and J. Bilalovikj, "Short-term wind speed prediction at Bogdanci power plant in FYROM using [30] an artificial neural network," *Int. J. Sustainable Energy*, vol. 38, no. 6, pp. 526–541, 2019. DOI: [10.1080/14786451.2018.1516668](https://doi.org/10.1080/14786451.2018.1516668).
- [30] H. H. Çevik, M. Çunkaş and K. Polat, "A new multi-stage short-term wind power forecast model using decomposition and artificial intelligence methods," *Physica A: Statistical Mechanics Its Appl.*, vol. 534, pp. 122177, Nov. 2019. DOI: [10.1016/j.physa.2019.122177](https://doi.org/10.1016/j.physa.2019.122177).
- [31] H. Liu, H. Wu and Y. Li, "Multi-step wind speed forecasting model based on wavelet matching analysis and hybrid optimization framework," *Sustainable Energy Technologies Assessments*, vol. 40, pp. 100745, Aug. 2020. DOI: [10.1016/j.seta.2020.100745](https://doi.org/10.1016/j.seta.2020.100745).